Elsevier Editorial System(tm) for Journal of Chromatography A

Manuscript Draft

Manuscript Number: JCA-16-1317R1

Title: Capillary methacrylate-based monoliths by grafting from/to γ-ray polymerization on a tentacle-type reactive surface for the liquid chromatographic separations of small molecules and intact proteins

Article Type: SI: Hi-Res Seps P and P

Keywords: Capillary High Performance Liquid Chromatography; Organic polymer monoliths; Monolith morphology; Biomolecule separation

Corresponding Author: Professor. francesco gasparrini, Full Professor

Corresponding Author's Institution: Università La Sapienza

First Author: Patrizia Simone

Order of Authors: Patrizia Simone; Giuseppe Pierri; Donatella Capitani; Alessia Ciogli; Giancarlo Angelini; Ornella Ursini; Gennaro Gentile; Alberto Cavazzini; Claudio Villani; francesco gasparrini, Full Professor

***Cover letter**

Dear Editor,

we are pleased to send you the revised version of the manuscript JCA-16-1317R1 that includes corrections suggested by reviewers. Additions and changes have been marked in red in the revised text.
We are grateful to the reviewers for appreciations and many positive comments that reward long work. Their suggestions offer us the opportunity to improve the paper making it more appealing for readers.

1. Grammar mistakes and English deficiencies were checked and modified as suggested.

2. The title and highlights have been modified to be more appropriate.

3. New literature references were added in according to the comments of reviewers (12,13,14,17,47,66,67).

4. Finally, other requests, such as those concerning the details of van Deemter plots and others (i.e. comments # 20-23-31 from Reviewer 3) are so trivial that they are no longer presented in research papers. They would render the text unnecessary long, wasting valuable journal space.

A detailed point-by-point (in red) reply for the principal points raised by each Reviewer is provided in a separate file.

Response to reviewers

Reviewer #1:
The manuscript entitled "Capillary polymethacrylate monoliths by innovative grafting from/to <gamma>-ray polymerization on a tentacle-type reactive surface for the HPLC of small molecules and intact proteins" authored by Gasparrini et al. is interesting in the sense that good separation efficiency is reported for both large biomolecules and small molecules. Generally, the Gasparrini group delivers high quality separations, and this is another demonstration of outstanding performance. Please allow me to make a critical comment (see comment 26); possibly adding some of the requested discussion raises the quality even more.
With respect to the publication in the Journal of Separation Science by the authors earlier this year, also discussing polymethacrylate monoliths prepared via gamma-ray polymerization, there are enough new elements in the current work to merit publication in JCA. Possibly the authors see some possibilities to condense the manuscript at some places and the manuscript requires a major improvement of the English language.

Comments
1. The grammar / English language should be thoroughly improved throughout the manuscript. For example:
- Title: I would recommend to have this checked by a native English speaker. It sounds very unnatural. We have changed the Title into “Capillary methacrylate-based monoliths by grafting from/to γ-ray polymerization on a tentacle-type reactive surface for the liquid chromatographic separations of small molecules and intact proteins”
- Also in lines 30-32 have syntax errors and are difficult to read. We have changed the whole sentence
- lines 33-35: Copolymerization "xxx" was generated "xxx". Corrected
- line 36: The morphology have been 'deeply' investigated. Corrected
- line 38-40 need revision (also the term reproducibility is incorrectly used throughout the manuscript; it is likely the authors mean repeatability). Corrected
- Please note that I only mention English deficiencies in the abstract. Please carefully check the manuscript. Checked

2. Keywords: <gamma>-ray polymerization and proteins are words in the title and thus not really required to be keywords. Corrected

3. General: put all Latin abbreviations and symbols in italics, check throughout manuscript. Checked

4. General: Check hyphenation throughout manuscript: microwave-assisted polymerization, free-radical process, flow-rate range, reversed-phase mode, etc. Checked

5. General: Please avoid the use of psi, but use SI units such as MPa (please adapt) Corrected

6. Line 71-72: add relevant references. We added references # 12,13,14

7. Line 78: implement the sensitivity? Syntax. Corrected

8. Line 109: from a morphological viewpoint Corrected

9. Line 111: Not all readers might be familiar with cross-polarization magic angle spinning NMR, write in full. We have added a text line explaining the meaning of the acronym

10. Line 118-119: "Supporting devices to protect the capillary columns" is quite vague, specify. We added the part number of the devices

11. Line 133: Origin of the monolithic column? We added this information

12. Line 148: Everhart-Thornley detector: perhaps it is clearer if you mention backscattered electrons + secondary electrons. We added this information

13. Line 179: USA Corrected

14. Lines 201-208, merge with lines 209-231 to avoid too much repetition Corrected

15. Line 256-257: it not only affects dimension and distribution of pores, but also of the globules. Please correct Corrected

16. Line 307: replace regime by range Corrected

17. Line 317: replace "tenths and tens" with an actual range. In line with a restyling process of manuscript we rephrased the sentence: “It has been previously shown that 1H NMR may be successfully applied for investigating the pore size distribution in mesoporous materials.”

18. Line 344-345: subscript is missing. Corrected

19. Figure 4: C is not mentioned in the caption. Perhaps a and b can be shown on the same graph. Corrected

20. Figure 5: the decimal separator seems to be a comma instead of a point Corrected

21. Line 386-389: your statement is not supported by what is seen in the SEM images. I would expect a larger difference in morphology given this substantial difference in backpressure/permeability. Were the monoliths also studied at the level of the macropores (e.g., via MIP) to confirm your statement? Perhaps some remarks about homogeneity could be included in the discussion regarding the difference in efficiency also. We tried to study the monoliths by MIP, but the results were not conclusive. We experienced some practical difficulties due to the low mechanical stability of the larger monolith required for the MIP measurements. A comment on the macropores size and homogeneity as obtained by SEM measurements was added in text.

22. Line 403. Provide proper statistics to justify that the fit is indeed good: "best numerical values of the fitted coefficients A, B and C are reported in table 2." We changed the sentence “in the optimal values corresponding to the minima of curve are reported in table 2”

23. Change header 3.6 (correct reproducibility). Corrected

24. Correct grammar line 474 (it is not "due to its high efficiency" the column is tested.) Corrected

25. Please place the results in perspective with results published in literature for peptides (Vaast et al Journal of Chromatography A, Volume 1374, 29 December 2014, Pages 171-179 and Journal of Chromatography A, Volume 1304, 23 August 2013, Pages 177-182) and intact proteins (Eeltink et

al Journal of Chromatography A, Volume 1218, Issue 32, 12 August 2011, Pages 5504-5511). We added some comments in the text relating to the new literature references #66 and 67.

26. The performance of the monoliths presented in impressive for the separation of small molecules, which is generally not achieved by other research groups. But the main question is: (1) why do your monoliths perform so well (is it better homogeneity or are there no surface diffusion/gel porosity effects and why not?) and (2) if the monoliths perform so much better for small molecules does this mean that the performance of large molecule separations is also better. Discussion on these aspects is very much appreciated!
We have not addressed these points in the paper, especially the relationship, if any, between the observed efficiency for small and large (bio)molecules. At this point, any comment would be speculative and we are planning to deeply investigate the interesting subject in a near future.

27. General comment: improve figure quality (4, 5, 6, 9).
- labels on x and y axis, sometimes the font/size, sometimes the content!.
- check the units.
- check if appropriate scale are used (van Veemter curves: x-axis 5-6 mm/s does not show data points, kinetic plots y axis should be adjusted (there is no data in 10-1 and 10-2 range and 10-4 to 10-5 range, so please do not show this range). Corrected

28. Grammar last 2 highlights should be improved. Corrected

Reviewer #2:
Summary
This work encompasses synthesis of poly(lauryl methacrylate-co-1,6-hexanediol dimethacrylate) monolithic columns in capillary diameters (75 µm, 200 µm and 250 µm i.d.) with a view to developing suitable materials for reversed-phase LC separation of small molecules, and to reinforce the suitability of the approach by demonstrating biomolecule separations. The novelty of the work is in the pre-treatment of capillary to allow a "grafting-to" approach to be used for anchoring the <gamma>-ray initiated monolithic co-polymer to the surface. While no direct comparison to columns prepared using conventional pre-treatment procedures has been made within this work, the material has been structurally characterized (IR, solid state NMR, cryogenic NMR & SEM), compared to a thermally-initiated equivalent (using AIBN), with a number of chromatographic experiments with small and large molecules also shown. Isocratic chromatographic comparison centers around evaluation of newly-synthesized materials against a column packed with 5 µm C18-functionalized particles in identical dimensions to the monolithic columns. Some further examples of biomolecule separations are shown in the gradient mode with high-resolution MS (Orbitrap).

The monolith prepared is primarily novel due to the pre-treatment process used. Previous publications from this group (refs [17] & [43]) contain extensive examples of peptide and protein separations including peak capacity calculations. Thus, the biomolecule work is of secondary value, except that the best material is shown to demonstrate very similar characteristics as the same stationary phase material synthesized with a conventional pre-treatment process from previous publications. However, the performance for small molecule separations is excellent and shows some behavior that is contrast to previously-published materials of similar origin. Specifically the retention-dependence of plate height seems to be almost non-existent, which is a major problem for most organic polymer monoliths used for analytical chromatography of small molecules.

There are some details missing from technical aspects of the work that I believe need to be addressed before publication. This includes a full explanation of the correction of plate height data for the chromatographic comparison (including the strange behavior of the packed column in terms

of efficiency). I believe that the work is actually most relevant to studying monolith formation and points toward interesting properties of the monolith derived from the combination of monomers and initiation used in this study (as best shown by small molecule HPLC experiments). This could be further built upon by the authors in the current work, although it is actually distinct from the goal of improving performance for biomolecule analysis. Some comparison of the performance of the new column (gamma-M1) and the new silanization procedure used should be made with that from previous publications for completeness and relevance to this special issue (Section 3.9/conclusions).

In order to avoid excessive length of the paper, the readers can easily compare the performance of new and old columns by refereeing to the previous publications.

Overall, the work is scientifically very interesting.

Title
The columns synthesized are described only as "polymethacrylate" - this is maybe a little bit unclear given the huge range of methacrylate monomers and that have been used for monolith synthesis. Methacrylate-based would be a better description throughout (e.g. PS-DVB is not described as "polystyrene monolith). We have changed the Title into "Capillary methacrylate-based monoliths by grafting from/to γ-ray polymerization on a tentacle-type reactive surface for the liquid chromatographic separations of small molecules and intact proteins"

Highlights:
- "Methacrylate-based", or more specific ("poly(lauryl methacrylate-co-1,6-hexanediol dimethacrylate)" would be better for the first highlight.
- "Both thermal and radiolytic polymerization were employed"
- "…SEM, and NMR cryoporosimetry"
- "Up to 102,000 plates/m were obtained…" - here would be a good opportunity to highlight the lack of dependence of performance upon retention for small molecules (see later comments).

We changed the Highlights accordingly, emphasizing the performances for both small molecules and proteins

Abstract
Line 41: has "reproducibility" been assessed here? Unless a different user, location, or instrument was the focus of this part of the study, then it is "repeatability" - e.g. batch-to-batch, column-to-column, run-to-run, interday… etc. Please choose accordingly. Changed
Line 42: again, "methacrylate-based" would be better here. Changed

Introduction
Line 60: silica- and polymer-based monoliths represent the majority of materials used by the analytical community, and commercial availability, but they are not the only types. It would be better to say that two of the most important groups are based on inorganic silica-based chemistry, and those derived from organic monomers. Changed
Line 64: "They are most commonly obtained by a single-step…" Changed
Line 70: "…suitable for high efficiency separations of large biomolecules,…" Changed
Line 73: "…preparation and, consequently, monolithic…"
Lines 77-78: "…used to implement the sensitivity of large molecules…" does not make sense. Please revise. Changed
Line 79: "The majority of recent developments have been…" Changed
Line 84: "microwave-assisted polymerization process."
Line 85: missing comma after "photo-induced" Changed

Line 87: "…methods) have also emerged as reviewed recently by Svec…" Changed
Line 89: "mold" or "confinement" would be better terminology than "holder"
Line 90: "…requires access to <gamma>-ray…"
Line 93: "…to reduce the possibility of bed heterogeneity (e.g. void spaces close to the wall)." Changed
Lines 94-95: The entire mechanical stability of the "frit-less" monolith is compromised without efficient adhesion to the capillary wall, this is the major point as emphasized in line 96. This has been resolved for fused silica and for PEEK confinements, so I don't see that this is an ongoing issue for "reproducibility" of separations exactly. Some commercially-available columns are housed in stainless steel in analytical dimensions and are not chemically anchored to the wall, but suitable separation repeatability is obtained as the "single particle" is confined using the column end-fittings. Some revision of this sentence is needed.

We agree with this comment and we deleted the sentence related to the mechanical stability, being not a general issue.

Line 105: "…permits the generation of a so-called …" Changed
Line 106 "covalently-anchored" Changed
Lines 112-113: The chromatographic (kinetic) performance of these columns…" - ("kinetic behavior" is not a clear description) Changed

Experimental
The tryptic digest procedure should be described separately to the chemicals section. Changed
Please provide a table with both polymerization (m1 & m2) mixtures specified in w/w %, or state clearly that these were identical in the text.
Please see lines 206-207.

Line 138: …spectra were measured at 100.13 MHz…" Changed
Line 147: "…analysis was performed on…" Changed
Line 155: "methanol-D4" Changed
Line 174-177: which peak width was used (half-height)? How were plate height values corrected? Please provide detailed examples in the supporting information. Please show an example of an uncorrected, and corrected plate height curve for uracil and a retained analyte for all 3 columns. It is somehow surprising that the efficiencies recorded on the packed, C18 column increase with retention, unlike the monolith, which cannot be attributed to extra column effects as column volumes, and retention factors are very similar.
The width at half-heigh was used for measuring the plate number without any correction (sentence inserted now in the text, Instrumentation, line 183). So the efficiency was estimated from the total band droadening (instrumental plus column) and only the linear velocity values have been corrected. The increase of efficiency with retention observed on the paked column is under investigation by a separate project, and is not the focus of the present work.

Line 190 (and throughout): should be "cytochrome c" (no capital) Changed
Line 205: "…a thermally-initiated monolith…" Changed
Line 220: were monomers first purified/de-inhibited or used straight of the bottle?
Lines 222-224: This sentence is back-to-front. It should be rearranged. Changed
Line 228: Was this a forced-air oven, a water bath, or a still air oven,…? Please specify. We added experimental details in the experimental section. line 228
Line 238: "in the reversed-phase mode" Changed
Line 241: "uracil" not "uracile" Changed
Line 247: "…were evaluated using the kinetic plot…" Changed

Results and Discussion
Line 266: "…the monolithic column was washed …" Changed
Line 269: "A comparable result (99%) was…" Changed
Lines 272-273: how is degradation of the polymer assessed? Some explanation is needed here. This could be quite a significant factor in the internal structure of the outer regions of monolith globules, which may have affected chromatographic behaviour of small molecules.

In the early stages of our research, we prepared monolithic columns using a gamma-ray exposure exceeding 40kGy (data not shown in this manuscript) and we recorded high back-pressure values and low efficiency for these columns. So we estimated the 40kGy dose as the optimum value taking also into account that the total conversion is reached in these conditions.

Line 291: "highly repeatable" - to be consistent with terminology Changed
Line 292: "… firmly bound to the inner…" Changed
Line 297: "…was used as an "octopus-like"… Changed
Line 302: "methacrylate-based" Changed
Lines 308-309: "… taken at magnification levels of 800, 10 000, and 30 000 …" Changed
Line 322: "… based on the phenomena of freezing point depression of the confined liquid with respect to…" Changed
Line 326: "it has also been demonstrated…" Changed
Line 330: Using benzene here is a very interesting experiment, as such a small probe molecule can sample much of the polymer free volume at the surface regions of globules where the degree of crosslinking is lower. The finding of a narrow pore size population in the thermally-initiated monolith, but not in the gamma-ray initiated one is particularly interesting. The lack of very small pores that can be sampled by the benzene in the M1 monolith points toward a difference in the properties of the polymer network. Some further experiments with different monolith types would be very interesting for future work to confirm this behavior in relation to chromatographic mass transfer experiments. We agree with the comments of the reviewer

Line 370: "without suffering measurable compression" - monoliths are axially compressible, but the quality of anchoring to the wall and operating at lower HPLC pressures minimizes these effects. Wall detachment can even occur at the head of capillary columns as the bed becomes compressed under high pressure, but this may not be observed as a strong trend in pressure/flow plots. Changed

Lines 398: It would have been better to use a higher retention factor for the kinetic plot experiments as the Supporting information chromatograms indicate that there was an issue with the packed column as efficiency increases significantly (~30%) with retention (unlike the monoliths). Again, the corrected and uncorrected data should be made transparent here, as over-correction of plate height values can render such results meaningless. See comments on point: lines 174-177

Line 408: "…for high speed and high efficiency separations…" Changed

Line 414: "inspection" Changed

Lines 417-419: see later comments on retention-dependence. A useful reference for comparison is: J. Chromatogr. A: 1358 (2014): 165. See comments on point: lines 174-177
Line 420: Please confirm that this is reproducibility or repeatability throughout the work (I believe it is the latter): (http://goldbook.iupac.org/R05305.html) Changed with "repeatability"

Line 430: "approximately 1%." Changed

Line 434: missing comma before "but" Changed
Line 439: "The Poppe plot…" Changed
Line 443: "…they both allow high efficiency values to be achieved in shorter times…" Changed
Line 448: so they visually resemble a conventional van Deemter…" Changed

In section 3.7, the role of smaller particles should also be mentioned based on what is commercially-available and shown in literature (including kinetic plots). Even will outperform the monoliths described here without a need for extremely high pumping pressures (aka UPLC). These can be packed into capillary columns and offer better overall performance for practical separations. We agree with the comments of the reviewer about the performance of 3 µm particles. However, since all the comparison in this work have been done with the 5 µm particles, we would like to keep the same comparison throughout the paper, and avoid to mention smaller of different formats for the packed column.

Lines 470-471: This is a speculative observation, but an understandable one. Taking the tabulated data (Table S1), one can calculate that the thermally-initiated polymer offers 18-31% higher retention for the probe solutes than the gamma-initiated one. If one assumes 100% conversion of monomers, and essentially the same phase ratio for each column (as supported by the almost equivalent total porosity values (Table 2), then what is responsible for this difference? The hydrophobicity of the columns should be the same - same monomers, same composition… It must relate to the ability of solutes (analytes) to interact with the stationary phase based on structure at the molecular level. i.e. as the probe solute is the same in each case, then how is the molecule partitioned/adsorbed onto/into the globules, and how are they different? Interestingly, styrenic polymer monoliths in analytical form offer much higher retention than silica-based, C18 modified columns of similar dimensions (Figure 2 from http://www.sciencedirect.com/science/article/pii/S0021967314010486).

The only explanation we can offer is related to a small but significant difference in surface area between the two otherwise identical monoliths. This is in part indicated by the bimodal pore size distribution for the thermal monolith, with a population centred around 2.5 nm (see section 3.4). However, this point needs further investigations and we do not want to anticipate here any conclusion that is not fully supported by experimental results.

In future work, it would be extremely interesting to examine the nanostructural properties of the two monoliths (e.g. An. Chem., (2013), 85: 5645) as the performance difference between the two fully-converted monoliths examined here is substantial. The SEM reveals perhaps a more uniform and spherical pore system for the gamma ray-initiated polymer, which may also be reflected in the internal crosslinking density uniformity of globules.

If these are uncorrected efficiency values, then Figure S3 (lower panel) is possibly the best isocratic separation of small molecules on a "pure" (i.e. not a hybrid material), 100%-converted organic polymer monolith that I have seen. Total plates/m is not a particularly useful chromatographic metric for synthesis of new monoliths unless it is provided for a wide range of analytes, and (even better) for a range of mobile phase conditions (i.e. flow rates & compositions). This should (in my opinion) be a standard expectation for similar studies. For a discussion of these points, see lines 174-177.

This is supported in Figure S2, which demonstrates a lack of retention-dependent performance for up to k = 2.9 at over 4.5 mm/s (t_0 ~ 1.1 min, presumably). This is remarkably better than for styrenic materials (despite manifold efforts to modify the materials with complex procedures) and

could indicate a fundamental difference in mass transfer (e.g. partitioning) processes due to differences in the nanostructure of the polymer network (e.g. polymer free volume, cross-linking density at the outer regions of globules, surface diffusion…). Moreover, a comparison with Figure 10a from http://www.sciencedirect.com/science/article/pii/S0021967310007910 indicates much better behavior than that of established poly(EDMA-co-BuMA) materials has been achieved - i.e. increasing retention does not diminish performance for this new column.

Apart from studying the interaction of solvent and polymer network in the chromatographic environment, perhaps the nature of the polymerization also plays a role here (i.e. <gamma>-radiation instead of thermal), or the new modification for pre-treatment? There are some interesting experiments that could be followed up here in future work.

Line 474: "for the separation of intact proteins" Changed
Line 475: "…its low flow resistance allowed higher flow rates to be employed (in the order of 15 µL/min), that are suitable…" the flow range has been added
Line 481: "assignment" is misspelled Changed
Line 486: "low charge state signals" would be better Changed

Some further comparison to the authors' previous work is needed here. Are the new columns offering some improvement for biomolecule analysis? Has the synthetic approach used here (octopus-like silanization reagent) improved any aspects. Also, how does the performance compare to the efforts of other groups for biomolecule separations (e.g. see works from Eeltink et al)?
From the limited HPLC data accumulated so far on the γ-M1 monolith with biomolecules, we are not able to draw general conclusions about the real advantages, if any, of the new columns over the old ones. A detailed comparison of the different inner surface activation chemistry is beyond the scope of the present work, and will reported in a separate paper. See also the response to point 26 of reviewer #1.

Conclusions
The aspects centering around the chromatographic behavior of small molecules for the new columns shown here is very interesting, but it may not be an influence on the good performance for gradient separations of biomolecules. The chromatographic processes involved in these two situations (small molecule/isocratic; and proteins/gradient elution) do not demand the same properties from a stationary phase. Nevertheless, the columns prepared here (M1) seems to be suitable for both situations. It might be interesting to perform some isocratic experiments with biomolecules to better understand the mass transport, which is strong obscured by the use of solvent gradients. Some reference to improvements offered by the new silanization procedure used should also be included here and throughout. See previous point.

Reviewer #3:
The authors have investigated a series of polymethacrylate capillary monoliths synthesized with tentacle-type inner wall activation via both thermal and radiolytic polymerization approaches. The resultant monoliths were characterized by related assessment techniques (such as, IR, SEM and NMR, etc). Good efficiency was obtained in terms of chromatographic separation of both small molecules and large biomolecules. In general, the present work is novel and interesting, and it has an impact and adds to the knowledge base. Thus, I suggest it could be publishable after a minor revision. And here is the following comments list:

#1: Line 1-3 A predicate verb was devoid in the title. Besides, it's better not use the abbreviation in the article title. If insisted by the authors, the HPLC separation probably be somewhat more

appropriate than "HPLC". Moreover, the author didn't explain what does the "HPLC" stand for anywhere? We have changed the Title into “Capillary methacrylate-based monoliths by grafting from/to γ-ray polymerization on a tentacle-type reactive surface for the liquid chromatographic separations of small molecules and intact proteins”

#2: Line 36-38/109-111 I personally suppose both the FT-IR and 13C CPMAS NMR could not contribute to the data in terms of "morphology and porous structure". We agree with the comment

#3: Line 41 How you calculate and obtain the linear velocity of about 0.5 mm/sec?
Please see lines 369-370
#4: Line 59-60 "A relevant number of reviews"? "has been published" Changed

#5: Line 132-133 What material was contained in the "5-cm long capillary monolithic column (250 ?m I.D.)."? In addition, please also clarify the source of this column, homemade or commercially available? We added this information

#6: Line 148 "The Netherlands"? Changed

#7: Line 169 and 241 I assume the "uracile" should be uracil on account of misspelling. Corrected

#8: Line 179 "NL,USA"? Corrected

#9: Line 214 Please denote the full name of the "IPA" acronym. Changed

#10: Line 233 Probably length internal and diameter combinations is better than "internal diameter and length combinations" in terms of agreement with following (L. × 234 I.D.). Changed

#11: Line 239 Please illustrate how you get the viscosity value of <eta>= 0.72 cP in the case of ACN/H2O 60/40 v/v at 25°C?
We added the corresponding reference [47]

#12: Line 259-260 How the authors calculate the percentage and what's the unit for 40% and 30%?
We added this information

#13: Line 264-266 How long time for the <gamma>-M1 column completion, 20 h? It's better to show here as ?-M2 column for comparison. We added this information

#14: Line 267-269 Please clearly show how to calculate the "percent conversion", e.g., a formula.
We added this information

#15: Line 284-285 Please also assign the rest two peaks of 21 and 20 here. We added this information
#16: Line 334 It's better to more specify the so-called IT method/plot because there is limited introduction and explanation to this abbreviation throughout this article. Changed

#17: Line 366-367 Please unify the unit. We added this information

#18: Line 368-369 What's the meaning of unretained/unexcluded compound? Please indicate which compound and what does the L refer to as in the following equation.
We added this information

#19: Line 372-376 Please rearrange the equations in accordance with the Arabic numerals. Besides, all the units for each parameter should also be completely clear. We rearranged all equations in the text.

#20: Line 400-401 What's the corresponding volumetric flow rate scope for the provided linear velocity value range, besides, please also explain each parameter grapheme in the van Deemter equation. Flow rate range has been reported in the text

#21: Line 449-451 Could the authors clarify how these values were obtained? We modified the sentence.

#22: Line 463 What did "figure 4C" refer to and why the authors show "figure 4C" here? Moreover, please clearly interpret why the more permeable <DELTA>-M2 monolith possessed the higher retention factors than <gamma>-M1 monolith here? Figure 4C in this part of text was a mistake. Concerning the higher retention of thermal than radiolytic monolith, we introduce this sentence in the text: An explanation of this data can be found in the different distribution of mesopores (see figure 4c). In fact, for the thermal Δ-M2 monolith, the pore population centered at about 2.5 nm is indicative of a greater surface area, wich in turn can be related to higher retention ability. See also lines 459-465 in the revised text.

#23: Line 468-469 Regarding the "methylene selectivity", authors should also discuss the third C18 columns except from these two monolithic columns. What's more important, could the authors theoretically explicate why there was "methylene selectivity" for all these columns in detail?
We included C18 column in the discussion. Explanation of methylene selectivity was intentionally omitted, as it obviously stems from the hydrophobic contribution to retention offered by the aliphatic fragments of the stationary phases.

#24: Line 472 Please check the X-axis title. done

#25: Line 487-490 The corresponding figure number was not assigned in the text although I assume it should be Figure 9. What's worse, the limited data information could be drawn from the given TIC figure. Consequently, it seems somewhat exaggerated for its top-down proteomic analysis application as mentioned in current section sub-title.
We changed the sub-title of section in “Capillary LC-MS of complex peptide sample”

#26: Line 494 Easy? I don't think it's an easy preparation approach to macroporous polymeric monoliths because the authors also mentioned "<gamma>-ray sources are expensive and need dedicated laboratory" in Line 91. We removed the word “easy”

#26: Line 496-497 After reading through this article, it's still hard to get the point of the apparent advantage for this more tedious silanization approach compared with the relatively simple but also efficient traditional route using more accessible silanization reagent.
We would like to point out that the new silanization procedure has the same number of steps of the traditional route, and that the silanization reagent is commercially available. The merits of the new route are detailed in section 3.2.

#27: Line 507 The authors didn't show sufficient data proving the monoliths' potential application in both top-down aforementioned in subtitle of section 3.9 and bottom-up proteomic analysis field.
See comment 25

#28: Line 517 Please unify the format for all references. Besides, please also recheck the references.

For instance, the reference [19] is not a review paper actually.
Corrected

#29: Line 697-698 Where is the missing (c) then? Caption has been completed

Comments on the SI part:

#30: Please check the serial number for Page 8. Corrected

#31: In Figure S1, please annotate what does the star marks refer to and it's also very important to fully assign and deeply discuss all the spectra in the main text or SI. Corrected

#31: As for Table S1, it's better for the authors distinctly show the equations for parameters' calculation in order to enhance article's readability, especially for those potential beginner readers.
See general comments at the beginning of this document (point # 4).

Highlights

- Capillary methacrylate-based monoliths were synthesized with tentacle-type inner wall activation
- Both thermal and radiolytic polymerization were employed
- Monoliths were characterized by FT-IR, solid state NMR, NMR cryoporosimetry, and SEM
- High efficiencies for separations of small molecules in isocratic mode and proteins in gradient elution were achievable.
- Thermal and radiolytic monoliths were compared in terms of morphology and chromatographic behaviours.

Highlights

- Capillary polymethacrylate monoliths were synthesized with tentacle-type inner wall activation
- Both thermal and radiolytic polymerization was employed
- Monoliths were characterized by FT-IR, solid state NMR, SEM, NMR cryoporosimetry
- Up to 102000 plates/meter were obtained in RP separations of alkylbenzenes
- Morphology and efficiency of thermal and radiolytic monoliths were compared

Capillary methacrylate-based monoliths by grafting from/to γ-ray polymerization on a tentacle-type reactive surface for the liquid chromatographic separations of small molecules and intact proteins.

Patrizia Simone[1], Giuseppe Pierri[1], Donatella Capitani[2], Alessia Ciogli[1], Giancarlo Angelini[2], Ornella Ursini[2], Gennaro Gentile[3], Alberto Cavazzini[4], Claudio Villani[1], Francesco Gasparrini[1,*]

(1) Dipartimento di Chimica e Tecnologie del Farmaco, Sapienza Università di Roma, P. le Aldo Moro 5, 00185 Roma (Italy)
(2) Istituto di Metodologie Chimiche, Area della Ricerca di Roma del CNR, Monterotondo Stazione, 00016 Roma (Italy)
(3) Istituto per i Polimeri Compositi e Biomateriali, Consiglio Nazionale delle Ricerche, Via Campi Flegrei 34, 80078 Pozzuoli (Italy)
(4) Dipartimento di Scienze Chimiche e Farmaceutiche, Università di Ferrara, via L. Borsari 46, 44121 Ferrara, Italy

***Corresponding author:** Francesco Gasparrini

E-mail address: francesco.gasparrini@uniroma1.it

Tel: +39 0649693124

Abstract

Capillary methacrylate-based monoliths were prepared for the high performance liquid chromatography (HPLC) separation of both small molecules and large biomolecules. An efficient grafting from/to synthetic approach was adopted introducing a network of activated sites in the inner wall surface using the new silanization agent (N-trimethoxysilylpropyl)-polyethylenimine. Copolymerization of lauryl methacrylate monomer and 1,6-hexanediol dimethacrylate cross-linker in the presence of porogenic solvents was obtained under continuous γ-ray exposure with high conversion yield.

The morphology and porous structure of the resulting monoliths have been ~~deeply~~ investigated by ~~Fourier transform infrared spectroscopy (FT-IR), solid state ^{13}C CPMAS NMR~~ Scanning Electron Microscopy (SEM) and ^{1}H NMR cryoporosimetry. By ~~a detailed~~ chromatographic investigation, the new capillary columns attested high kinetic performance (with efficiency larger than 100,000 theoretical plate/meter for small molecules at optimum mobile phase linear velocity of about 0.5 mm/sec) and also excellent mechanical stability and repeatability.

The new methacrylate-based monolithic capillary columns have been successfully employed for efficient reversed-phase separation of intact proteins and peptides.

Keywords: Capillary High Performance Liquid Chromatography; Organic polymer monoliths; Monolith morphology; Biomolecule separation.

1. Introduction

Monolithic materials are versatile adsorbents widely employed in separation science, sample preparation and as supports for flow-through applications (e.g. heterogeneous catalysis, ion-exchange, solid-phase extraction, etc.) [1-4]. Interest around their preparation and applications has been rapidly growing in recent years. Some reviews about the use of monoliths as separation media for analytical chromatography have been published [5-10]. Two of the most important groups of monoliths are based on inorganic silica chemistry, and those derived from organic monomers. Silica-based monoliths consist of a bi-continuous mesoporous skeleton as result of the sol-gel preparation method designed by Tanaka in the 90s [11]. On the other hand, polymeric organic ones have a normally globule-like backbone. They are most commonly obtained by a single-step polymerization process starting from a bulk mixture of monomers, cross-linkers (difunctional monomers) and porogens. In both cases, monoliths are characterized by a single-body mesoporous structure with interconnected channels (flow-through pores).

Thanks to the possibility of modulating the skeleton thickness with respect to the width of the flow-through pores, monoliths combining high efficiency and high permeability can be prepared. They have been proven to be particularly suitable for high efficiency separations of large biomolecules, which are excluded by the mesoporous network and do not experience the usually slow mass transfer therein [12-14]. A further considerable advantage also includes the simplicity of *in-situ* preparation and, consequently, monolithic chromatographic columns of virtually any geometry and shape can be easily prepared. This flexibility allows to overcome the constraints related to both packing and miniaturization of the conventional particle-based chromatographic columns. Nowadays, polymer monolithic column technology has been successfully applied for the HPLC separation of large molecules such as intact proteins, synthetic polymers, peptides [15-18], and used to improve the sensitivity when directly interfaced to UV absorbance detection or MS [19-20]. The majority of recent developments have been focused on the optimization of their morphology to achieve a better efficiency and enhanced mass transport of solutes, as reported by Nischang [21]

and Shen et al. [22]. Different monomers (acrylamide, acrylate, methacrylate, vinylbenzene), cross-linkers and monomer/cross-linker ratio have been evaluated to induce a control of pore dimensions and to improve efficiency and biocompatibility [23-32]. New solvent systems as ionic liquids have also been introduced in a microwave-assisted polymerization process [33]. Polymerization of active precursors involves a free radical process mainly thermal or photo-induced, but several less common free radical polymerization techniques (γ-ray, electron beam, living processes, polycondensation methods) have also emerged as reviewed by Svec [34]. Among them, γ-ray induction does not require an initiator and the polymerization can be carried out at room temperature in almost any confinement, including the stainless steel columns usually employed for the preparation of HPLC columns [35-36]. On the other hand, the use of this powerful technology requires access to γ-ray sources, which are expensive and need dedicated laboratory. In the preparation of monolithic columns, a crucial step is the strong adhesion of the polymer backbone to the inner walls of the holder where the polymerization is performed (e.g., the capillary column), to reduce the possibility of bed heterogeneity and void spaces close to the wall. Without an efficient adhesion, the quality of separation in terms of efficiency and reproducibility is compromised. ~~So is the mechanic stability of monoliths.~~ To obtain a strongly tethered organic monolith, usually, the capillary surface is subjected to a two-step treatment: the so-called etching step firstly makes available the silanols groups present on the inner wall; then, the superficial grafting procedure (silanization step) introduces on the silanols the reactive units that will be covalently embedded into the monolithic skeleton during the polymerization process. Usually, acidic and alkaline solutions are alternately used in the etching procedure, while the surface modification is carried out by anchoring 3-((trimethoxysilyl)propyl) methacrylate [37-42].

In this work, we present an innovative grafting synthetic approach on a multisite tentacle-type inner-wall activated surface obtained by using (N-trimethoxysilylpropyl)-polyethylenimine as silanization agent and methacrylic anhydride. The “octopus-like” surface modification permits the generation of a so-called *grafting from/to* polymerization process since the covalently anchored

active units (vinyl groups) take part to the free radical polymerization happening in the bulk phase, possessing the active moieties of precursors, both monomers and cross-linkers. The new methacrylate-based monoliths are extensively characterized from a morphological viewpoint by employing a series of advanced techniques including FT-IR (Fourier transform infrared spectroscopy), solid state ^{13}C CPMAS NMR (Cross-Polarization Magic Angle Spinning Nuclear Magnetic Resonance, SEM (Scanning Electron Microscopy) and ^{1}H NMR cryoporosimetry. The chromatographic performance of these columns for the reversed-phase separation of small molecules and intact proteins is discussed.

2. Experimental

2.1 Chemicals and samples

Fused-silica capillary tubings of 0.250, 0.200 and 0.075 mm I.D. (0.375 mm O.D.) with a polyimide outer coating were purchased from Polymicro Technologies (Phoenix, AZ, USA). Dorica Supporting devices (figure S1) to protect the capillary columns were from Avantech Group s.r.l (Angri, SA, Italy). Azoisobutyronitrile (AIBN), acetonitrile (ACN), trifluoroacetic acid (TFA), lauryl methacrylate (LMA), 1,6-hexanediol dimethacrylate (HDDMA), *tert*-butyl alcohol, 1,4-butanediol, tetrahydrofuran (THF), methacrylic anhydride, pyridine, sodium hydroxide (NaOH), hydrochloric acid (HCl), ammonium bicarbonate, uracil, phenol, benzaldehyde, nitro-benzene, benzene, toluene, ethyl-benzene, n-propyl-benzene, n-butyl-benzene, n-pentyl-benzene as well as lysozyme from chicken egg white, α-lactalbumin from bovine milk, β-lactoglobulin B from bovine milk, carbonic anhydrase from bovine erythrocytes, core histones from calf thymus were purchased from Sigma-Aldrich (St. Louis, MO, USA). Porcine trypsin was purchased from Promega (Madison, WI, USA). (N-trimethoxysilylpropyl)-polyethylenimine from United Chemical Technologies (Bristol, PA, USA) was used as a silanization reagent.

2.2 Digestion procedure of plasma protein mixture.

Plasma protein mixture was solubilized in 25 mM ammonium bicarbonate and subsequently trypsin was added to give an enzyme-to-substrate ratio of 1:50 (w/w). The digest was kept at 37°C overnight, after which the tryptic peptide mixture was acidified with 5% formic acid to terminate the digestion. Desalting and preconcentration of the peptide mixture was performed using a 5-cm long capillary monolithic column (250 μm I.D.). The column was methacrylate-based built with the same polymerization mixture as reported in following 2.4 section.

2.3 Instrumentation

Diffuse Reflectance Infrared Fourier Transform (DRIFT) and transmission IR (potassium bromide pellets or liquid paraffin dispersion) spectra were recorded on a Jasco 430 Fourier transform (FT) IR spectrometer (Jasco Europe, Cremella, Italy) at a resolution of 4 cm^{-1}.

Solid-state ^{13}C CPMAS NMR spectra were measured at 100.13 MHz on a Bruker Avance III spectrometer. The spin rate was 8000 Hz. The contact time for the cross-polarization was 1 ms, the recycle delay was 3 sec, and the ^{1}H $\pi/2$ pulse was 3.2 μs. The cross-polarization was performed by applying the variable spin-lock sequence RAMP-CPMAS [43], the RAMP was applied on the ^{1}H channel, and during the contact time the amplitude of the RAMP was increased from 50 to 100% of the maximum value. High-power proton dipolar decoupling was carried out using the Spinal-64 scheme [44]. The decoupling field was 140 kHz. Spectra were acquired with a time domain of 1,024 data points were zero filled and Fourier transformed with 2,048 data points, applying exponential multiplication with 8 Hz line broadening.

SEM analysis was performed on a FEI Quanta 200 FEG SEM (Eindhoven, NL) at 30 kV acceleration voltage and with an Everhart-Thornley (secondary electron and back-scattered electron) detector. Before the analysis, samples were mounted onto SEM specimen holders and sputter-coated with a gold-palladium alloy.

Wide line ^{1}H NMR spectra of C_6H_6 saturated networks were recorded on a Bruker Avance spectrometer operating at the proton frequency of 300.13 MHz. A variable temperature unit equipped with an N_2 flux from a pressurized line was used in the temperature range 298-190 K.

158 Spectra were recorded by co-adding 32 transients with a recycle delay of 60 sec, the ^1H $\pi/2$ pulse
159 was 6 μs. The temperature was carefully calibrated using a 4% methanol in methanol-D4 standard
160 sample. In the investigated range of temperature, the calibration was carried out recording the
161 chemical shift separation between the OH resonance and the CH_3 resonance of methanol.
162 ^1H wide line NMR spectra were deconvoluted using the DM2011 software package. The intensity
163 of NMR signal, the chemical shift, and the width at half-height of C_6H_6 and network resonances
164 were used as input parameters in the deconvolution procedure. The area of the resonance of C_6H_6
165 obtained from the deconvolution procedure was reported *vs* 1000/T to obtain IT plot.
166 Chromatographic measurements, under isocratic conditions, were performed on a Waters CapLC
167 system (Waters, Milford, MA, USA) equipped with a home-made injection system consisting in a
168 VICI pneumatic actuator (Valco, Houston, TX, USA) controlled by a home-made electronic time
169 switch, a 2996 ternary CapLC pump and a MicroUVis 20 UV detector (Carlo Erba, Milan, Italy)
170 with an home-made 20 nL perpendicular flow cell. In its optimized configuration, the UV flow cell
171 is characterized by a path length of 150 μm, an illuminated volume of ≈ 20 nL, a connecting tube
172 (150 μm, O.D.) with inner diameter of 30 μm, length of 40 cm and a total volume of 283 nL. Peak
173 variance from peak-width at half-height measured (σ^2) for uracil in ACN/H_2O 60/40 *v/v* was
174 ranging from 130 to 1000 nL^2 at the applied flow rate from 0.5 to 3.0 μL/min; while in the same
175 flow rate regime the second central moment ($\mu'_{2,ex}$) was ranging from 200 to 1300 nL^2 [45]. In all
176 measurements the time constant of 0.10 sec was used. Chromatographic data were collected with a
177 sample rate of 100 Hz and processed using MassLynx 4.1 (Waters, Milford, MA, USA) and Clarity
178 (LabService Analytica, BO, Italy) software. All reported data of column pressure drop, column
179 permeability and retention were obtained after correction for the system pressure drop and t_0-time
180 measured by removing the column from the system and by a direct connection of a tube (150 μm,
181 O.D.; 30 μm, I.D.; 40 cm, L.) between the pump and the UV cell. The width at half-heigh was used

for measuring the plate number without any correction (N/m, according to European Pharmacopeia, EP).

Separations of biomolecules were performed using an UltiMate3000 RSLC nanoLC (Dionex, Amsterdam, NL) equipped with binary separation capillary flow pump, a ternary loading pump, a thermostatted column compartment and a variable wavelength detector with a 7.0 nL Z-shaped flow cell. Time constant and the data collection rate were set to 0.10 sec and 40 Hz respectively. Chromatographic data were performed with Chromeleon 6.8 (Dionex, Sunnyvale, CA, USA).

MS detection was performed on an Exactive Orbitrap (Thermo Fisher Scientific, San Josè, CA, USA), equipped with a Standard Electrospray Source. The MS instrument was operated at a resolution of 100,000 in positive ESI mode with a sheath gas flow of 15 units, an auxiliary gas of 5 units, a spare gas of 4 units, a spray voltage of 2.3 kV, a capillary voltage of 30 V, a capillary temperature of 275 °C, a tube lens voltage of 240, and a skimmer voltage of 25 V. One microscan was accumulated with a maximum injection time of 100 msec. The MS parameters were optimized in the range of 500-2500 m/z by infusing a solution of 8.0 µM cytochrome c (cat.no C-2506 from Sigma-Aldrich) in H_2O/ACN/TFA (80/20/0.05 *v/v/v*), at resolution of 30,000-100,000 with a syringe pump at a flow rate of 10.00 µL/min.

Mass spectra were collected and processed using Xcalibur software and deconvoluted mass spectra were obtained by using Xtract and ProMass software (Thermo Fisher Scientific).

2.4 Preparation of organic monolithic capillary columns

The monolith was generated by copolymerization of LMA monomer and HDDMA cross-linker as reported in [46], where it was also demonstrated that this stationary phase provides excellent mechanical stability and permeability and very high peak capacity values, making it suitable for separation of intact proteins in miniaturized chromatographic systems. For comparative purposes, a thermal monolith (Δ-M2) was also prepared by adding to the same polymerization mixture a free radical initiator (azobisisobutyronitrile) in amount of 1% w/w with respect to monomers.

In the present work, capillary columns were prepared following an innovative multi-step procedure. **1st step** (capillary etching): the inner wall of the fused-silica capillary is treated in a static mode with an aqueous solution of 1 M NaOH for 3 h at 120°C, washed with water, treated with an aqueous solution of 0.1 M HCl for 3 h at 70°C and finally washed with consecutive 5 ml portions of water and methanol and then dried under nitrogen flow.

2nd step (multisite tentacle-type inner wall activation): the pre-treated capillary is filled with a solution of 10% *v/v* (N-trimethoxysilylpropyl)-polyethylenimine in 2-propanol and heated at 70°C for 12 h. After cooling, it is washed with a solution of MeOH/H_2O 60/40 *v/v* containing 10% *v/v* of acetic acid. The filled capillary is then heated at 50°C for 3 h and washed with consecutive 5 ml portions of methanol and THF. By using a syringe, the capillary is filled with a solution of 20% *v/v* of methacrylic anhydride in pyridine/acetonitrile 1/1 *v/v*, heated at 40°C for 2 h, and finally washed with acetonitrile.

3rd step (preparation of the polymerization solution): monomers and cross-linkers were filtered on alumina before use. The polymerization mixture is prepared in a glass vial by admixing monomer, cross-linker and porogens and then degassed by helium sparging for 5 minutes at room temperature. Through a slight argon pressure (ranging from 20 to 60 psi, depending on the diameter and length of the capillary), it is then introduced into the pre-treated capillary. The ends of the capillary columns are finally sealed by silicon rubber.

4th step (polymerization): filled capillaries are placed inside a Gammacell and irradiated at room temperature with a total dose of 40 kGy, with a dose rate of about 2 kGy/h. Instead, for Δ-M2 monolith, filled capillaries are positioned in a still air oven heated at a temperature of 50°C and maintained for 24 h. Lastly, all capillaries are connected to an apparatus for micro-HPLC and washed with acetone (about 50 column dead volumes) under constant pressure (5 or 10 MPa, depending on the diameter and length of the capillary).

2.5 Chromatographic set-up

In this study, monolithic columns with different length and internal diameter combinations (L. × I.D.) were investigated: 300 and 250 mm × 0.25 mm; 1100 mm × 0.200 mm; 250 mm × 0.075 mm. In order to compare kinetic and thermodynamic performance, we used a homemade packed 5 µm silica Hypersil C18 100 Å capillary column with the same internal diameter and length combinations of both polymethacrylate columns γ-M1 and Δ-M2 (300 × 0.25 mm L. × I.D.). Chromatographic characterization under isocratic elution was carried out in reversed-phase mode using ACN/H_2O 60/40 *v/v* as eluent (η= 0.72 cP at 25°C, [47]) with a flow rate range extending from 0.250 to 10.00 µL/min at a temperature of 25°C and UV detection at 214 nm. A test mixture of 10 compounds (**1.**uracil, **2.**phenol, **3**.benzaldehyde, **4.**nitrobenzene, **5.**benzene, **6.**toluene, **7.**ethylbenzene, **8.**propylbenzene, **9.**butylbenzene and **10.**pentylbenzene) was used to evaluate the efficiency and retentivity of the columns. van Deemter plots were obtained by fitting the experimental efficiency data of benzaldehyde as representative analyte for each column. Data fitting of the experimental points to van Deemter equation was performed using Origin 8.0 software and kinetic performance of the different columns were evaluated using the kinetic plot method [48,49] setting the maximum backpressure of the HPLC system at 40 MPa and the viscosity of the mobile phase at 0.72 cP. Due to the higher chromatographic efficiency of radiolytic monolithic columns (up to 102,000 plate/meter vs. roughly 50,000 plate/m of Δ-M2), these have been employed in capillary-HPLC analysis coupled with high resolution mass spectroscopy (cap-HPLC-HRMS) under RP-gradient conditions.

3. Results and Discussion

3.1 Conversion efficiency, FT-IR and ^{13}C-CP-MAS NMR investigations

The polymerization mixture, reaction conditions and the monomer/porogen volume ratio affect the morphology of the monoliths in terms of dimension, distribution and shape of pores, and therefore the chromatographic performance of the final columns. In our first experiments (data not shown) we observed the best kinetic performance when the monomer content in the polymerization mixture

was decreased from 40% (high density range) [31] to 30% (medium density range), where percentage values refer to the volumetric content of monomers and cross-linkers respect to the total volume of polymerization mixture. Maintaining the medium density monomers/porogens ratio, γ-M1 monolith was obtained from the optimized polymerization mixture as reported in a previous publication [50].

Quantitative data on monomer conversions were collected using 50 × 10 mm (L. × I.D.) stainless-steel columns filled with the polymerization mixtures and irradiated with a total dose of 40 kGy in 20 h (γ-M1 column) or alternately heated at 50°C for 24 h (Δ-M2 column). After completion of the polymerization process, the monolithic column was washed *in-situ* using an HPLC pump, dried and removed from the column. Percent conversion, calculated as % weight of monolith/weight of monomers and cross-linkers, was almost quantitative at total doses of 40 kGy, and close to 98% at 20 kGy. A comparable result (99%) was obtained for thermal triggered polymerization. A total dose of 40 kGy was chosen throughout our study as the best compromise between completeness of the polymerization, acceptable reaction time, and minimum degradation of the formed polymer monolith due to an excessive exposure to γ-radiation. Radiolytic and thermal polymer monoliths also showed superimposable ^{13}C CP-MAS (figure 1) and FT-IR (figure S2) spectra, proving either way the achievement of a complete monomer and cross-linker conversion into a saturated polymeric structure. By careful analysis of ^{13}C CPMAS spectra, the peaks of vinyl carbons at about 136 and 125 ppm observed in spectra of monomers are no longer present in the spectrum of the cross-linked monolith (see figure 1). Carbon resonances of methylene (2), methyl (3) and quaternary (1) carbon atoms of the main polymeric backbone are observed at 54.7, 15.2, and 44.0 ppm respectively [51]. The resonance of the carbonyl carbon (4) is observed at 176 ppm. The peak of methylene carbons (5, 10) having an oxygen as first neighbour and belonging to the bridge between polymeric backbones is observed at 63.9 ppm. At the same frequency the peak of methylene carbon (11) having an oxygen as first neighbour and belonging to the side chain is also observed. The peak of terminal methyl (22) is observed at 13.6 ppm, whereas the peak of methylene

carbon (21) having the terminal methyl as a first neighbour is found at 22.3 ppm, and the peak of the methylene carbon (20) having the methyl as a second neighbour is possibly observed at 31.5 ppm. All other methylene carbons (6-9, and 12-19) resonate between 25 and 30 ppm.

FIGURE 1

3.2 Multisite tentacle type inner wall activation

While bulk polymerization of monomers and cross-linkers induced by γ-radiation is straightforward and highly repeatable, polymerization inside HPLC capillaries poses the additional challenge of obtaining a uniform monolith firmly bound to the inner capillary walls in order to provide a monolithic column. Indeed, any discontinuity of the polymer monolith, causing preferential path flow of the mobile phase, negatively affects the chromatographic performance (wall effect).

In this work, we introduced a new silanization procedure to covalently anchor the monolith to the capillary inner wall surface. After standard etching procedures, the (N-trimethoxysilylpropyl) polyethyleneimine was used as an "octopus-like" silanization agent, affording a flexible and multisite reactive surface. The following introduction of unsaturated units with methacrylic anhydride completes the activation of capillary inner walls (figure 2). Then, the polymerization proceeds in a *grafting from/to* fashion, simultaneously from the methacrylate moieties anchored on the polyethyleneimine coating and from methacrylate precursors (monomers and crosslinkers) in the bulk. Thus a *monobody* methacrylate-based column is generated as a highly homogeneous three-dimensional polymeric network firmly anchored to the column inner walls.

FIGURE 2

3.3 Morphological characterization of monoliths

SEM yielded valuable structural details on the final polymeric monoliths in the micrometer range. Morphology of the two different γ-M1 and Δ-M2 methacrylate-based monoliths is illustrated by SEM micrographs taken at 800, 10000 and 30000 magnifications (figure 3). The composite media reveal the familiar cauliflower internal structure of porous monoliths featuring micro globules of relatively uniform size agglomerated into larger clusters. Inspection of low magnification SEM

micrographs (figure 3, left) reveals that in both cases the monolith was covalently bond to the silica surface and no cracks were present, confirming an effective and efficient *grafting from/to* process.

FIGURE 3

3.4 ^{1}H NMR cryoporosimetry

It has been previously shown that ^{1}H NMR may be successfully applied for investigating the pore size distribution in mesoporous materials [52-57]. Before performing measurements, the porous matrix must be saturated with a liquid probe which must be a non solvent for the porous solid matrix. Then the area of the ^{1}H resonance of the liquid probe must be reported *vs* temperature from room temperature down to low temperature (IT plot). The obtained IT plot represents the fingerprint of a porous network without requiring any model of the shape of pores [58]. This approach is based on the phenomena of freezing point depression of a confined liquid with respect to the freezing temperature of the bulk liquid [59]. Based on the Gibbs-Thompson equation, the freezing phenomena of a liquid confined into restricted volumes may give information on the pores size distribution. Many porous materials such as zeolites and other silicates have been studied with ^{1}H NMR cryoporosimetry [55]. In these studies, it has also been demonstrated that the pores size distribution obtained by ^{1}H NMR cryoporosimetry compares well with distributions obtained by N_2 adsorption measurements [52]. In particular, with this method the pores structure of water-, benzene-, and cyclohexane-saturated porous silica has been mapped out [52]. We used benzene as a liquid probe to map out the porous structure of our networks.

At room temperature ^{1}H spectra of benzene-saturated networks showed a rather sharp resonance of benzene and a very broad resonance of the solid matrix. By lowering the temperature, the benzene resonance progressively broadened and decreased in intensity. ^{1}H spectra were deconvoluted to obtain the area of both resonances. According to the IT method, the integral of the benzene resonance was reported *vs* 1000/T. IT plots of sample γ-M1 (a) and Δ-M2 (b) are shown in figure 4. Note that the steep transition of signal intensity observed in both samples between 283 and 278 K was due to the freezing of bulk C_6H_6. At lower temperatures, sample γ-M1 showed just one

intensity transition whereas sample Δ-M2 showed two transitions. These intensity transitions are due to freezing of benzene confined in pores with a different average dimension. In figure 4 these transitions are evidenced with arrows.

The intensity of a liquid probe confined in a porous matrix is related to X=1000/T through the equation [52]:

$$I(X) = \sum_{i=1}^{N} \frac{I_{0i}}{2}\left[1 + \exp\left[\frac{X_{ci} - X}{\Delta_i \sqrt{2}}\right]\right] \quad (1)$$

where I_{0i}, X_{ci} and Δ_i represent the intensity, the inverse transition temperature ($X_{ci}=1000/T_{ci}$) and the width of the temperature distribution curve of phase i, I(X) represents the total amount of the liquid probe confined in pores at the inverse temperature X=1000/T and N is the number of temperature transitions. Note that, for a very sharp transition Δi tends to 0, while the broader the transition the higher the Δ_i value. Parameters I_{0i}, X_{ci} and Δ_i were obtained fitting the experimental data to equation 1, see table 1, the uncertainty on data reported in the table varies between 6 and 10%.

According to the literature [52], differentiating equation 1 with respect to X and using an equation which correlates the freezing point temperature depression ΔT of the confined liquid to the pore radius (Rp) it is possible to obtain the pore size distribution:

$$\frac{dI}{dRp} = \sum_{i=1}^{N} \frac{I_{0i}}{1000 K_b \Delta_i \sqrt{2\pi}} (XT_0 - 1000)^2 \exp\left[-\left(\frac{X - X_{ci}}{\Delta_i \sqrt{2}}\right)^2\right] \quad (2)$$

where T_0= 278.5 K is the freezing temperature of bulk benzene, and K_b= 1107 K was obtained from literature data [52].

Using equation 2 and the parameters reported in table 1, the pore size distributions for samples γ-M1 and Δ-M2 was obtained (see figure 4 c).

It is worth noticing that sample γ-M1 showed one asymmetric distribution centered at about 13 nm, whereas sample Δ-M2 showed a bimodal distribution with a sharp peak centered at about 2.5 and a broad asymmetric peak centered at about 8 nm in a relative amount of 36 and 64%.

Table 1

FIGURE 4

3.5 Permeability and Efficiency

The plot of the backpressure generated by the column (ΔP_c, MPa) against the mobile phase linear velocity (μ_0, mm/s) is reported on the left side of figure 5 for the two monolithic columns (300 mm × 0.250 mm, L × I.D.) and a Hypersil C18 packed column (particle size 5 µm, 300 mm × 0.250 mm, L × I.D.). Linear velocities are calculated as ratio of the elution time, t_0, of the unretained compound uracil and the column length, L ($\mu_0 = L/t_0$). The linear dependence of ΔP_c on μ_0 (linear regression R^2s > 0.999) show that the monolithic bed is stable without suffering measurable compression. From these plots, column permeability K_0 [60] can be calculated according to:

$$K_0 = \frac{\mu_0 \eta L}{\Delta P_c} \qquad (3)$$

where η is the viscosity of the solvent ~~and L the column length~~. Alternatively, the specific permeability K_{SF} is given by:

$$K_{SF} = \frac{\eta L \Phi}{r^2 \pi \Delta P_c} \qquad (4)$$

where Φ is the flow rate and r the radius of column. Both the permeability and the specific permeability values obtained by linear regression analysis of ΔP *vs* μ_0 (or ΔP *vs* Φ) plots are summarized in table 2.

FIGURE 5

The maximum pressure drop recorded at the highest linear velocity was around 15 and 6 MPa for γ-M1 and Δ-M2 monolith columns respectively, while a value of 17 MPa was found for the packed column.

The total porosity of monolithic columns can be calculated as:

$$\varepsilon_T = K_{SF}/K_0 \quad (5)$$

Total porosities of monolothic columns were very similar each other and significantly higher than that of the packed particle column. On the other hand, the larger permeability of Δ-M2 (K_0 = 18.0 * 10^{-14} m^2) compared to γ-M1 (K_0 = 7.0 * 10^{-14} m^2) is due to the larger globule of the thermal monolith with the distribution centered at 0.78 µm and therefore the pore size, as evidenced by SEM analysis (figure S3). In order to compare hydrodynamic properties of monolithic and packed columns, permeability-equivalent particle diameter d_{perm} [61] was calculated using the following equation:

$$d_{perm} = \sqrt{1000 \times K_{SF}} \quad (6)$$

where 1000 is the so-called flow resistance value for a typical packed column with external porosity of about 0.4. Thus the permeability of γ-M1 monolith is comparable to that of a column packed with spherical particles of about 7 µm diameter, while the permeability of Δ-M2 is higher and comparable to that of a column packed with 11.5 µm particles (table 2). The differences in d_{perm} and globule distribution provide also different efficiency as attested by van Deemter inspection.

Table 2

~~To evaluate the kinetic performance of both monolithic and packed columns,~~ The traditional efficiency-linear velocity plots were built using benzaldehyde as retained solute (figure 5, right) in ACN/H_2O 60/40 *v/v* at 25°C, by changing the eluent linear velocity from 0.12 to maximum 5.00 mm/s (or 0.25-10 µl/min range). The data were therefore fitted to the van Deemter equation:

$$H = \mathrm{A} + \frac{B}{\mu_0} + C \times \mu_0 \quad (7)$$

and the optimal working values corresponding to the minima of the plots are reported in table 2.

The minima of the van Deemter curves for the monolithic columns were H_{min} = 9.8 and 18.9 µm for γ-M1 and Δ-M2 respectively; on the other hand, the packed column exhibited H_{min} of 12.9 µm. Observation of figure 5 shows that the van Deemter curve of γ-M1 monolithic column is

characterized by a less steep C branch portion due to a lower mass transfer resistance in the porous structure. It is thus more suitable for high speed and high efficiency separations. The almost twice larger C-term of Δ-M2 column compared to that of γ-M1 one, despite the fact that the two monoliths have identical chemistry, points out that the radiolitic polymerization procedure favours the achievement of a more microglobular structure with monodispersed porosity centered at 13 nm (figure 4). γ-M1 monolith showed higher flow-resistance than Δ-M2 thermal monolith and enhanced kinetic behavior (lower C and H_{min} values) even compared with the Hypersil C18 column packed with 5 µm particles. An extended van Deemter inspection of the behavior of these two columns is reported under Supporting Information (figure S4) where van Deemter curves for a series of low molecular weight compounds with capacity factors between 0.30 and 7.0 (γ-M1 monolith) and between 0.7 and 8.8 (Hypersil C18, 5 µm column) are presented. Remarkably, efficiency of about 100,000 plate/meter was observed also using 75 µm I.D. monolithic column, which represents a considerable result in the practice of miniaturized nano liquid chromatography (figure S5).

3.6 Repeatibility and long-term stability

Run-to-run and batch-to-batch repeatibility of γ-M1 monolith were assessed by performing a series of injections of a sample of four standard proteins in gradient elution mode. The comparison of retention time of the test compounds in a series of five consecutive injections were characterized by a relative standard deviation (RSD) smaller than 1% for each component (figure S6-A) showing therefore a very high run-to-run reproducibility. Analogous results (RSD <1%) were obtained also in terms of batch-to-batch reproducibility, as detailedly described under Supporting Information (figure S6-B). Finally, the long term column stability was also investigated by considering the separation of the same mixtures of core histones from calf thymus on a new monolithic column and on the same column after 1000 runs (see Supporting Information, figure S6-C): even in this case, the RSD of retention times of corresponding peaks was approximately 1%.

3.7 Kinetic Plots

The Kinetic Plot Method (KPM) is a powerful tool to predict the theoretical highest performance achievable in the shortest possible time at the maximum pressure allowed by the system [48,49]. KPM is useful not only to evaluate column quality, but also to compare the kinetic performance of columns with different size and morphology. In this study, kinetic plots were calculated by assuming 41 MPa as the maximum HPLC backpressure and 0.72 cP as the mobile phase viscosity. Specific permeabilities, as well as values of μ_0 and H were obtained experimentally (see before). The resulting t_0/N *vs.* N (so-called Poppe plot) and t_0/N^2 *vs.* N plots are shown in figure 6A and B respectively. The Poppe plot [62] (figure 6A) reflects the separation speed that can be achieved at the maximum pressure. Fastest separations are located in the bottom left corner, while analysis with high resolution and efficiency are in the top-right of the plot. Given the comparable C-terms of γ-M1 and C18 silica-based columns, significantly lower than that Δ-M2 monolith (see table 2), they both allow high efficiency values to be achieved in shorter times than for the thermal monolith. Since, the higher permeability of monolithic columns allows using longer columns at a fixed maximum pressure and higher plate numbers can be achieved only with monoliths. For lower N values, essentially the same length of γ-M1 and Hypersil C18 columns is required, while the Δ-M2 would need to be twice as long. Figure 6B shows impedance time t_0/N^2 *vs.* N plots. In these plots, N-values (*x*-axis) are in reversed order with respect to Poppe plots, so visually they resemble conventional van Deemter plots. The radiolitic γ-M1 monolith shows the widest linear velocity range of use, mainly in the low-to-medium region where its achievable efficiencies are dominant.

FIGURE 6

3.8 Thermodynamic investigation: retention and methylene selectivity

Hydrophobicity of the columns was investigated through the retention behavior of a series of small molecules (phenol, benzaldehyde, nitrobenzene, benzene, toluene, ethylbenzene, propylbenzene, butylbenzene and pentylbenzene) in reversed-phase mode (using ACN/H_2O, 60/40 *v/v*). Figure 7 compares the chromatograms obtained with the three columns. First of all, one may notice the different behavior in terms of retention between the two monolithic columns. As detailedly reported

under Supporting Information (table S1)**,** retention factors *(k*s*)* measured on the Δ-M2 monolith were systematically larger than those of the radiolitic column. While the chemical composition of the two monoliths is identical, the detailed geometrical orientations of the hydrophobic chains and of the polar ester fragments could be different for the two materials (prepared at different temperatures). Retention data for the same test solutes seem to indicate a larger accessibility of the aalkyl chains for the thermal Δ-M2 compared to the radiolithic γ-M1 monolith. In addition , for the thermal Δ-M2 monolith, the pore population centered at about 2.5 nm is indicative of a greater surface area, wich in turn can be related to higher retention ability. Moreover, we estimated the methylene selectivity (α_{CH2}) of the stationary phases, i.e. their ability to distinguish between two compounds differing by a single methylene group [63-65], using the homologous series of alkylbenzenes from toluene to pentylbenzene. In figure S7, the plots of the logarithmic retention factors *vs.* the incremental number of methylene groups are reported. This study evidenced that the three stationary phases have essentially the same α_{CH2} (log*k vs* n_{CH2} plots having the same slope). On the other hand, γ-M1 showed a ~~remarkably~~ lower value of the y-intercept compared to those of Δ-M2 and of C18 Hypersil, which reflects a lower contribution of the aromatic end group to retention.

FIGURE 7

3.9 Capillary LC-MS of complex peptide sample

It is well known that polymer monoliths show great potential for reversed-phase gradient separation of biomolecules and also peptides [66-67]. In fact, the highly porous structure allows the use of long columns to improve separation efficiency and in addition, permits higher flow rates (in the order of 15 µL/min), that are suitable for coupling the column to MS instruments through standard electrospray ionization (ESI) interface.

A standard mixture of four intact proteins was analyzed on the γ-M1 column (250 × 0.250 mm L. × I.D.) using gradient elution and high resolution MS detection (figure 8). As it can be seen from the figure, total ion current chromatogram showed additional peaks (with respect to UV signal). The

identification of each peak was obtained by deconvolution of multicharged MS spectra as reported under Supporting Information (figure S8). Briefly, two different lyzozyme isoforms (**p1-a**, **p1-b**) and two impurities of carbonic anhydrase (**i-1**, **i-2**) could be identified (see table S2 of Supporting Information). Signals due to multiply charged ions (z always higher than +13) were recorded with high isotopic resolution (about 40-50,000) for all proteins except than **p4**. The exact mass of **p4** (29022.8 Da) was determined by artifact-free deconvolution of low charge state signals using ProMass. The separation of real complex peptide sample was also performed by using a very long column (110 cm × 200 μm, L × I.D.) directly interfaced to the mass spectrometer via standard ESI source. Maintaining the column pressure at an acceptable level, plasma proteins digest was well separated with a 50 min gradient at 7 μL/min flow rate (figure 9).

FIGURE 8

FIGURE 9

4. Conclusions

Gamma radiation offers an alternative route for an *in-situ* preparation of macroporous polymeric monoliths suitable as separation media in analytical chemistry. In this work, to obtain the capillary column by γ ray polymerization, we proposed an innovative "tentacle type" *grafting from/to* approach producing multisite, flexible grafted reactive surface of capillary inner walls. ~~Monolithic stationary phases for capillary HPLC characterized by chromatographic efficiencies > 102,000 plate/m were prepared under continuous γ ray exposure.~~ The chemical, physical and morphological properties of lauryl methacrylate-1,6-hexanediol dimethacrylate co-polymer were investigated by FT-IR, solid state ^{13}C CPMAS NMR, SEM and ^{1}H NMR cryoporosimetry. The evaluation of chromatographic performance, using a set of small molecules, has revealed high efficiency and high resolution power, together with low flow resistance and very significant mechanical stability. Moreover, the fabricated columns demonstrated excellent repeatability with RSD values for run-to-run and column-to-column below 1%. Efficient separation of intact proteins and peptides by LC-

MS on lauryl polymethacrylate-based monolithic capillary columns was realized, demonstrating their potential use in separation of complex peptide samples.

Acknowledgments

This study was supported by PRIN contract n. 2012ATMNJ_003 and by Sapienza Università di Roma contract n. C26H13ZSR4. The authors thank Mr. Enrico Rossi as technical assistant in NMR measurements. The authors are also grateful to Avantech group s.r.l (Angri, SA, Italy) for the supporting devices of capillary columns.

The authors have declared no conflict of interest.

5. References

[1] P. A. Levkin, S. Eeltink, T.R. Stratton, R. Brennen, K. Robotti, H. Yin, K. Killeen, F. Svec, J. M. Fréchet, Monolithic porous polymer stationary phases in polyimide chips for the fast high-performance liquid chromatography separation of proteins and peptides, J. Chromatogr. A 1200 (2008) 55-61.

[2] F. Svec, Less common applications of monoliths: Preconcentration and solid-phase extraction, J. Chromatogr. B 841 (2006) 52-64.

[3] Y. Hu, Y. Fan, G. Li, Preparation and evaluation of a porous monolithic capillary column for microextraction of estrogens from urine and milk samples online coupled to high-performance liquid chromatography, J. Chromatogr. A 1228 (2012) 205-2012.

[4] A. Nordborg, E.F. Hilder, Recent advances in polymer monoliths for ion-exchange chromatography, Anal. Bioanal. Chem. 394 (2009) 71-84.

[5] G. Zhu, L. Zhang, H. Yuan, Z. Liang, W. Zhang, Y. Zhang, Recent development of monolithic materials as matrices in microcolumn separation systems, J. Sep. Sci. 30 (2007) 792-803.

[6] J. Urban, P. Jandera, Polymethacrylate monolithic columns for capillary liquid chromatography, J. Sep. Sci. 31 (2008) 2521-2540.

[7] R. Wu, L. Hu, F. Wang, M. Ye, H. Zou, Recent development of monolithic stationary phases with emphasis on microscale chromatographic separation, J. Chromatogr. A 1184 (2008) 369-392.

[8] G. Guiochon, Monolithic columns in high-performance liquid chromatography, J. Chromatogr. A 1168 (2007) 101-168.

[9] K.K. Unger, R. Skudas, M.M. Schulte, Particle packed columns and monolithic columns in high-performance liquid chromatography-comparison and critical appraisal, J. Chromatogr. A 1184 (2008) 393-415.

[10] F. Svec Y. Lv, Advances and Recent Trends in the Field of Monolithic Columns for Chromatography, Anal. Chem. 87 (2015) 250-273.

[11] H. Minakuchi, K. Nakanishi, N. Soga, N. Ishizuka, N. Tanaka, Octadecylsilylated porous silica rods as separation media for reversed-phase liquid chromatography, Anal. Chem. 68 (1996) 3498-3501.

[12] F. Gritti, W. Piatkowski, G. Guiochon, Study of the mass transfer kinetics in a monolithic column, J Chromatogr A 983 (2003) 51–71.

[13] F.C. Leinweber, U. Tallarek (2003) Chromatographic performance of monolithic and particulate stationary phases. Hydrodynamics and adsorption capacity. J Chromatogr A 1006 (2003) 207–228.

[14] A. Jungbauer, R. Hahna, Polymethacrylate monoliths for preparative and industrial separation of biomolecular assemblies, J Chromatogr A 1184 (2008) 62–79.

[15] R.D. Arrua, M. Talebi, T.J. Causon, E.F. Hilder, Review of recent advances in the preparation of organic polymer monoliths for liquid chromatography of large molecules, Anal. Chim. Acta 738 (2012) 738 1-12.

557 [16] E.C. Peters, M. Petro, F. Svec, J. M. Fréchet, Molded rigid polymer monoliths as separation
558 media for capillary electrochromatography. 2. Effect of chromatographic conditions on the
559 separation, Anal. Chem. 70 (1998) 2296-2302.
560 [17] Morphology and efficiency of poly (styrene-co-divinylbenzene)-based monolithic capillary
561 columns for the separation of small and large molecules Jens H. Mohr & Remco Swart & Christian
562 G. Huber Anal Bioanal Chem (2011) 400:2391–2402
563 [18] R. Shediac, S.M. Ngola, D.J. Throckmorton, D.S. Anex, T.J. Shepodd, A.K. Singh, Reversed-
564 phase electrochromatography of amino acids and peptides using porous polymer monoliths, J.
565 Chromatogr. A 925 (2001) 251-263.
566 [19] A. Premstaller, H. Oberacher, W. Walcher, A.M. Timperio, M. Zolla, J.P. Chervet, N.
567 Cavusoglu, N. van Dorsselaer, C. Huber, High-performance liquid chromatography-electrospray
568 ionization mass spectrometry using monolithic capillary columns for proteomic studies, Anal.
569 Chem. 73 (2001) 2390-2396.
570 [20] A. Vellaichamy, J.C. Tran, A. D. Catherman, J.E. Lee, J.F. Kellie, S.M.M. Sweet, L.
571 Zamdborg, P.M. Thomas, D.R. Ahlf, K.R. Durbin, G.A. Valaskovic, N.L. Kelleher, Size-sorting
572 combined with improved nanocapillary liquid chromatography-mass spectrometry for identification
573 of intact proteins up to 80 kDa, Anal. Chem. 82 (2010) 1234-1244.
574 [21] I. Nischang, Porous polymer monoliths: morphology, porous properties, polymer nanoscale gel
575 structure and their impact on chromatographic performance, J. Chromatogr. A 1287 (2013) 39-58.
576 [22] Y. Shen, L. Qi, L. Mao, Macroporous polymer monoliths with a well-defined three
577 dimensional skeletal morphology derived from a novel phase separator for HPLC, Polymer 53
578 (2012) 4128-4134.
579 [23] J. Urban, P. Jandera, P. Langmaier, Effects of functional monomers on retention behavior of
580 small and large molecules in monolithic capillary columns at isocratic and gradient conditions, J.
581 Sep. Sci. 34 (2011) 2054-2062.

582 [24] A. Nordborg, F. Svec, J.M. Fréchet, K. Irgum, Extending the array of crosslinkers suitable for
583 the preparation of polymethacrylate-based monoliths, J. Sep. Sci. 28 (2005) 2401-2406.
584 [25] S.H. Lubbad, M.R. Buchmeiser, Highly cross-linked polymeric capillary monoliths for the
585 separation of low, medium, and high molecular weight analytes, J. Sep. Sci. 32 (2009) 2521-2529.
586 [26] P. Jandera, M. Staňkova, V. Škeřikova, J. Urban, Cross-linker effects on the separation
587 efficiency on (poly)methacrylate capillary monolithic columns. Part I. Reversed-phase liquid
588 chromatography, J. Chromatogr. A 1274 (2013) 97-106.
589 [27] C. P. Bisjak, S. H. Lubbad, L. Trojer, G. K. Bonn, Novel monolithic poly(phenyl acrylate-co-
590 1,4-phenylene diacrylate) capillary columns for biopolymer chromatography, J. Chromatogr. A
591 1147 (2007) 46-52.
592 [28] C. P. Bisjak, L. Trojer, S.H. Lubbad, W. Wieder, G.K. Bonn, Influence of different
593 polymerisation parameters on the separation efficiency of monolithic poly(phenyl acrylate-co-1,4-
594 phenylene diacrylate) capillary columns, J. Chromatogr. A 1154 (2007) 269-276.
595 [29] A. Greiderer, L. Trojer, C. W. Huck, G. K. Bonn, Influence of the polymerisation time on the
596 porous and chromatographic properties of monolithic poly(1,2-bis(p-vinylphenyl))ethane capillary
597 columns, J. Chromatogr. A 1216 (2009) 7747-7754.
598 [30] L. Trojer, C. P. Bisjak, W. Wieder, G. K. Bonn, High capacity organic monoliths for the
599 simultaneous application to biopolymer chromatography and the separation of small molecules, J.
600 Chromatogr. A 1216 (2009) 6303-6309.
601 [31] S. Eeltink, J.M. Herrero-Martinez, G.P. Rozing, P. J. Schoenmakers, W.T. Kok, Tailoring the
602 morphology of methacrylate ester-based monoliths for optimum efficiency in liquid
603 chromatography, Anal. Chem. 77 (2005) 7342-7347.
604 [32] P. Aggarwal, J. S. Lawson, H. D. Tolley, M. L. Lee, High efficiency polyethylene glycol
605 diacrylate monoliths for reversed-phase capillary liquid chromatography of small molecules, J.
606 Chromatogr. A 1364 (2014) 96-106.

607 [33] B. Singco, C. L. Lin, Y. J. Cheng, Y. H. Shih, H. Y. Huang, Ionic liquids as porogens in the
608 microwave-assisted synthesis of methacrylate monoliths for chromatographic application, Anal.
609 Chim. Acta 746 (2012) 123-133.
610 [34] F. Svec, Porous polymer monoliths: amazingly wide variety of techniques enabling their
611 preparation, J. Chromatogr. A 1217 (2010) 902-924.
612 [35] Á. Sáfrány, B. Beiler, K. László, F. Svec, Control of pore formation in macroporous polymers
613 synthesized by single-step γ-radiation-initiated polymerization and cross-linking, Polymer 46
614 (2005) 2862-2871.
615 [36] B. Beiler, Á Vincze, F. Svec, Á. Sáfrány, Poly(2-hydroxyethyl acrylate-co-ethyleneglycol
616 dimethacrylate) monoliths synthesized by radiation polymerization in a mold, Polymer 48 (2007)
617 3033-3040.
618 [37] J. Courtois, M. Szumski, E. Byström, A. Iwasiewicz, A. Shchukarev, K. Irgum, A study of
619 surface modification and anchoring techniques used in the preparation of monolithic microcolumns
620 in fused silica capillaries, J. Sep. Sci. 29 (2006) 14-24.
621 [38] G.T.T. Gibson, S. M. Mugo, R.D. Oleschuk, Surface-mediated effects on porous polymer
622 monolith formation within capillaries, Polymer 49 (2008) 3084-3090.
623 [39] J. Vidič, A. Podgornik, A. Štrancar, Effect of the glass surface modification on the strength of
624 methacrylate monolith attachment, J. Chromatogr. A 1065 (2005) 51-58.
625 [40] B. Zhao, W.J. Brittain, Polymer Brushes: Surface-Immobilized Macromolecules, Prog. Polym.
626 Sci. 25 (2000) 677-710.
627 [41] R. Barbey, L. Lavanant, D. Paripovic, N. Schüwer, C. Sugnaux, S. Tugulu, H.A. Klok,
628 Polymer brushes via surface-initiated controlled radical polymerization: synthesis, characterization,
629 properties, and applications, Chem. Rev. 109 (2009) 5437-5527.
630 [42] S. Minko, S. Patil, V. Datsyuk, F. Simon, K. J. Eichhorn, M. Motornov, D. Usov, I. Tokarev,
631 M. Stamm, Synthesis of Adaptive Polymer Brushes via "Grafting To" Approach from Melt,
632 Langmuir 18 (2002) 289-296.

633 [43] G. Metz, X. Wu, S. O. Smith, Ramped-amplitude cross polarization in magic-angle-spinning
634 NMR, J. Magn. Reson. A 110 (1994) 219-227.
635 [44] G. Comellas, J.J. Lopez, A.J. Nieuwkoop, L.R. Lemkau, C.M. Rienstra, Straightforward,
636 effective calibration of SPINAL-64 decoupling results in the enhancement of sensitivity and
637 resolution of biomolecular solid-state NMR, J. Magn. Reson. 209 (2011) 131-135.
638 [45] F. Gritti, G. Guiochon, On the extra-column band-broadening contributions of modern, very
639 high pressure liquid chromatographs using 2.1 mm I.D. columns packed with sub-2 μm particles, J.
640 Chromatogr. A 1217 (2010) 7677-7689.
641 [46] P. Simone, G. Pierri, P. Foglia, F. Gasparrini, G. Mazzoccanti, A.L. Capriotti, O. Ursini, A.
642 Ciogli, A. Laganà, Separation of intact proteins on γ-ray-induced polymethacrylate monolithic
643 columns: A highly permeable stationary phase with high peak capacity for capillary high-
644 performance liquid chromatography with high-resolution mass spectrometry, J. Sep. Sci. 39 (2016)
645 264–271.
646 [47] L.R. Snyder, J.J. Kirkland, J.W. Dolan, Introduction to Modern Liquid Chromatography
647 Willey, 2010, 3rd ed.
648 [48] G. Desmet, D. Clicq, P. Gzil, Geometry-independent plate height representation methods for
649 the direct comparison of the kinetic performance of LC supports with a different size or
650 morphology, Anal. Chem. 77 (2005) 4058-4070.
651 [49] D. Kotoni, A. Ciogli, C. Molinaro, I. D'Acquarica, J. Kocergin, T. Szczerba, H. Ritchie, C.
652 Villani, F. Gasparrini, Anal. Chem. 84 (2012) 6805-6813.
653 [50] G. Pierri, D. Kotoni, P. Simone, C. Villani, G. Pepe, P. Campiglia, P. Dugo, F. Gasparrini,
654 Analysis of bovine milk caseins on organic monolithic columns: an integrated capillary liquid
655 chromatography-high resolution mass spectrometry approach for the study of time-dependent
656 casein degradation, J. Chromatogr. A 1313 (2013) 259-269.
657 [51] F.A. Bovey, P.A. Mirau, NMR of Polymers, Academic Press, San Diego, California, 1996.

658 [52] E. W. Hansen, R. Schimdt, M. Stöcker, Pore Structure Characterization of Porous Silica by 1H
659 NMR Using Water, Benzene, and Cyclohexane as Probe Molecules, J. Phys. Chem. 100 (1996)
660 11396-11401.
661 [53] K. Overloop, L. Van Gerven, Freezing Phenomena in Adsorbed Water as Studied by NMR, J.
662 Magn. Reson. A101 (1993) 179-187.
663 [54] R. Schmidt, E.W. Hansen, M. Stöcker, D. Akporiaye, O.H. Ellestad, Water-Saturated
664 Mesoporous MCM-41 Systems Characterized by 1H NMR Spin-Lattice Relaxation Times, J. Phys.
665 Chem. 99 (1995) 4148-4154.
666 [55] D. Akporiaye, E.W. Hansen, R. Schmidt, M. Stöcker, Water-Saturated Mesoporous MCM-41
667 Systems Characterized by 1H NMR, J. Phys. Chem. 18 (1994) 1926-1928.
668 [56] E.W. Hansen, R. Schmidt, M. Stöcker, D. Akporiaye, Water-Saturated Mesoporous MCM-41
669 Systems Characterized by 1H NMR Spin-Lattice Relaxation Times, J. Phys. Chem. 99 (1995)
670 4148-4154.
671 [57] E.W. Hansen, M. Stöcker, R. Schmidt, Low-Temperature Phase Transition of Water Confined
672 in Mesopores Probed by NMR. Influence on Pore Size Distribution, J. Phys. Chem. 100 (1996)
673 2195-2200.
674 [58] D. Capitani, N. Proietti, F. Ziarelli, A.L. Segre, NMR Study of Water-Filled Pores in One of
675 the Most Widely Used Polymeric Material: The Paper, Macromolecules 35 (2002) 5536-5543.
676 [59] J.H. Strange, M. Rahman, E.G. Smith, Characterization of porous solids by NMR, Phys. Rev.
677 Lett. 71 (1993) 3589-3591.
678 [60] J. Grafnetter, P. Coufal, E. Tesarovà, J. Suchànkovà, Z. Bosakova, J. Sevcìk, Optimization of
679 binary porogen solvent composition for preparation of butyl methacrylate monoliths in capillary
680 liquid chromatography, J. Chromatogr. A 1049 (2004) 43-49.
681 [61] S. Eeltink, P. Gzil, W. T. Kok, P.J. Schoenmakers, G. Desmet, Selection of comparison criteria
682 and experimental conditions to evaluate the kinetic performance of monolithic and packed-bed
683 columns, J. Chromatogr. A 1130 (2006) 108-114.

[62] H. Poppe, Some reflections on speed and efficiency of modern chromatographic methods, J. Chromatogr. A 778 (1997) 3-21.

[63] J. Layne, Characterization and comparison of the chromatographic performance of conventional, polar-embedded, and polar-endcapped reversed-phase liquid chromatography stationary phases, J. Chromatogr. A 957 (2002) 149–164.

[64] N. Marchetti, L. Caciolli, A. Laganà, F. Gasparrini, L. Pasti, F. Dondi, A. Cavazzini, Fluorous affinity chromatography for enrichment and determination of perfluoroalkyl substances, Anal. Chem. 84 (2012) 7138–7145.

[65] M. Catani, R. Guzzinati, N. Marchetti, L. Pasti, A. Cavazzini, Exploring Fluorous Affinity by Liquid Chromatography, Anal. Chem. 87 (2015) 6854–6860.

[66] A. Vaast H. Terrynb, F. Svecc, S. Eeltink, Nanostructured porous polymer monolithic columns for capillary liquid chromatography of peptides, J Chromatogr A, 1374 (2014) 171–179.

[67] S. Eeltink, B. Wouters, G. Desmet, M. Ursem, D. Blinco, G. D. Kemp, A. Treumann, High-resolution separations of protein isoforms with liquid chromatography time-of-flight mass spectrometry using polymer monolithic capillary columns, J Chromatogr A, 1218 (2011) 5504–5511.

Figure captions

Figure 1. Solid state ^{13}C CPMAS NMR spectra of thermal (a) and radiolytic (b) monoliths. Assignement was discussed in the text.

Figure 2. Tentacle type inner wall activation and *grafting on-to* polymerization process.

Figure 3. SEM images of γ-M1 (top) and Δ-M2 (bottom) monoliths**.**

Figure 4. IT plots of sample γ-M1 (a) and Δ-M2 (b), solid lines through the experimental points were obtained fitting the experimental data to equation 1. (c) Pore size distribution of samples γ-M1 and Δ-M2 obtained from equation 2.

Figure 5. Pressure-linear flow velocity plots (left) and van Deemter plots (right) for columns containing ◓ γ-M1_300 mm × 0.25 mm monolith and ○ Δ-M2_300 mm × 0.25 mm monolith in comparison to ● Hypersil C18, 5 µm packed column (300 mm × 0.25 mm L. × I.D.). Eluent: ACN/H_2O 60/40 *v/v*, viscosity given as η = 0.72 cP at 25 °C. Uracil for permeability data, and benzaldehyde (*k*: 0.30 for γ-M1; *k*: 0.38 for Δ-M2 and *k*: 0.72 for Hypersil C18, 5 µm) for van Deemter inspection, were used as markers.

Figure 6. Poppe plot (top) and t_0/N^2 *vs.* N (bottom) for ethylbenzene. Columns: (◉) γ-M1_300 mm × 0.25 mm monolith, (●) Δ-M2_300 mm × 0.25 mm monolith and (●) Hypersil C18, 5 µm 300 mm × 0.25 mm**.** Mobile phase: ACN/H_2O 60/40, *v/v*; T_{col}: 25 °C. Maximum system pressure: 6000 psi.

Figure 7. Comparison of isocratic elution on γ-M1_300 mm × 0.25 mm (top), Hypersil C18, 5 µm 300 mm × 0.25 mm (middle) and Δ-M2_300 mm × 0.25 mm (bottom) by eluting a small molecules mixture. Mobile phase: ACN/H_2O 60/40 *v/v*; detection wavelength: 214 nm; flow rate: 1.0 µl/min. Results are expressed as theoretical plates per meter (N/m).

Figure 8. Total ion current chromatogram and UV traces of standard proteins mixture (**i-1** and **i-2.** impurity **1** and **2** of the carbonic anhydrase, respectively, **p1-a**. lysozyme isoform a, **p1-b.** lysozyme isoform b, **p2**. α-lactalbumin, **p3**. β-lactoglobulin, **p4**. carbonic anhydrase) on γ-M1_250 mm × 0.25 mm monolith. Mobile phases: (A) H_2O/ACN 95/5 + 0.1% TFA; (B) ACN/H_2O 95/5 + 0.1% TFA; 15 min gradient elution from 5% to 70% of mobile phase B; flow rate: 15 µL/min; T_{col}: 60 °C.

Figure 9. Total ion current chromatogram of plasma protein digest (CapHPLC-HRMS analysis).

Pre-Column: γ-M1 5 cm × 0.25 mm L. × I.D. Loading solvent: 0.1% aqueous trifluoroacetic acid; trapping time: 5 min; loading flow rate: 10 μL/min; Column: γ-M1_1100 mm × 0.200 mm L. × I.D. Mobile phases: (A) H_2O/ACN 95/5 + 0.1% TFA; (B) ACN/H_2O 95/5 + 0.1% TFA; gradient elution from 3% to 35% of mobile phase B in 40 min, from 35% to 50% in 1 min, from 50% to 70% in 4 min and finally hold for 5 min; flow rate: 7 μL/min; T_{col}: 60 °C.

Capillary polymethacrylate monoliths by innovative grafting from/to γ-ray polymerization on a tentacle-type reactive surface for the HPLC of small molecules and intact proteins

Patrizia Simone[1], Giuseppe Pierri[1], Donatella Capitani[2], Alessia Ciogli[1], Giancarlo Angelini[2], Ornella Ursini[2], Gennaro Gentile[3], Alberto Cavazzini[4], Claudio Villani[1], Francesco Gasparrini[1,*]

(1) Dipartimento di Chimica e Tecnologie del Farmaco, Sapienza Università di Roma, P.le Aldo Moro 5, 00185 Roma (Italy)
(2) Istituto di Metodologie Chimiche, Area della Ricerca di Roma del CNR, Monterotondo Stazione, 00016 Roma (Italy)
(3) Istituto per i Polimeri Compositi e Biomateriali, Consiglio Nazionale delle Ricerche, Via Campi Flegrei 34, 80078 Pozzuoli (Italy)
(4) Dipartimento di Scienze Chimiche e Farmaceutiche, Università di Ferrara, via L. Borsari 46, 44121 Ferrara, Italy

***Corresponding author:** Francesco Gasparrini

E-mail address: francesco.gasparrini@uniroma1.it

Tel: +39 0649693124

Abstract

An efficient grafting from/to synthetic approach on a highly activated tentacle-type multisite surface obtained thanks to a new silanization agent ((N-trimethoxysilylpropyl)-polyethylenimine) has been employed to prepare capillary polymethacrylate monoliths suitable for the chromatographic separation of both small molecules and large biomolecules. Copolymerization of lauryl methacrylate monomer and 1,6-hexanediol dimethacrylate cross-linker in the presence of porogenic solvents was generated under continuous γ-ray exposure with high conversion yield.

The morphology and porous structure of the resulting monoliths have been deeply investigated by Fourier transform infrared spectroscopy (FT-IR), solid state ^{13}C CPMAS NMR, Scanning Electron Microscopy (SEM) and ^{1}H NMR cryoporosimetry. In addition, a detailed chromatographic investigation of the new capillary columns has shown not only their high kinetic performance (with efficiency larger than 100,000 theoretical plate/meter for small molecules at optimum mobile phase linear velocity of about 0.5 mm/sec) but also excellent mechanical stability and reproducibility.

The new polymethacrylate-based monolithic capillary columns have been successfully employed for efficient reversed-phase separation of intact proteins and peptides.

Keywords: Capillary High Performance Liquid Chromatography; γ-ray polymerization; Organic polymer monoliths; Monolith morphology; Proteins

1. Introduction

Monolithic materials are versatile adsorbents widely employed in separation science, sample preparation and as supports for flow-through applications (e.g. heterogeneous catalysis, ion-exchange, solid-phase extraction, etc.) [1-4]. Interest around their preparation and applications has been rapidly growing in recent years. A relevant number of reviews about the use of monoliths as separation media for analytical chromatography has been published [5-10]. Depending on their nature, monoliths can be classified into two groups, inorganic silica-based and organic polymeric materials. Silica-based monoliths consist of a bi-continuous mesoporous skeleton as result of the sol-gel preparation method designed by Tanaka in the 90s [11]. On the other hand, polymeric organic ones have a globule-like backbone. They are obtained by a single-step polymerization process starting from a bulk mixture of monomers, cross-linkers (difunctional monomers) and porogens. In both cases, monoliths are characterized by a single-body mesoporous structure with interconnected channels (flow-through pores).

Thanks to the possibility of modulating the skeleton thickness with respect to the width of the flow-through pores, monoliths combining high efficiency and high permeability can be prepared. They have been proven to be particularly suitable for the high-efficient separation of large biomolecules, which are excluded by the mesoporous network and do not experience the usually slow mass transfer therein. A further considerable advantage also includes the simplicity of their *in-situ* preparation, consequently, monolithic chromatographic columns of virtually any geometry and shape can be easily prepared. This flexibility allows to overcome the constraints related to both packing and miniaturization of the conventional particle-based chromatographic columns. Nowadays, polymer monolithic column technology has been successfully applied for the HPLC separation of large molecules such as intact proteins, synthetic polymers, peptides [12-15], and used to implement the sensitivity when directly interfaced to UV absorbance detection or MS [16-17]. Most of recent developments have been focused on the optimization of their morphology to achieve a better efficiency and enhanced mass transport of solutes, as reviewed by Nischang [18] and Shen

et al. [19]. Different monomers (acrylamide, acrylate, methacrylate, vinylbenzene), cross-linkers and monomer/cross-linker ratio have been evaluated to induce a control of pore dimensions and to improve efficiency and biocompatibility [20-29]. New solvent systems as ionic liquids have also been introduced in a microwaves assisted polymerization process [30]. Polymerization of active precursors involves a free radical process mainly thermal or photo-induced but several less common free radical polymerization techniques (γ-ray, electron beam, living processes, polycondensation methods) are meanwhile emerged as reviewed by Svec [31]. Among them, γ-ray induction does not require an initiator and the polymerization can be carried out at room temperature in almost any holder, including the stainless steel columns usually employed for the preparation of HPLC columns [32-33]. On the other hand, the use of this powerful technology requires the access to γ-ray sources, which are expensive and need dedicated laboratory. In the preparation of monolithic columns, a crucial step is the strong adhesion of the polymer backbone to the inner walls of the holder where the polymerization is performed (e.g., the capillary column), to avoid the presence of heterogeneity and void spaces close to the wall. Without an efficient adhesion, the quality of separation in terms of efficiency and reproducibility is compromised. So is the mechanic stability of monoliths. To obtain a strongly tethered organic monolith, usually, the capillary surface is subjected to a two-step treatment: the so-called etching step firstly makes available the silanols groups present on the inner wall; then, the superficial grafting procedure (silanization step) introduces on the silanols the reactive units that will be covalently embedded into the monolithic skeleton during the polymerization process. Usually, acidic and alkaline solutions are alternately used in the etching procedure, while the surface modification is carried out by anchoring 3-((trimethoxysilyl)propyl) methacrylate [34-39].

In this work, we present an innovative grafting synthetic approach on a multisite tentacle-type inner-wall activated surface obtained by using (N-trimethoxysilylpropyl)-polyethylenimine as silanization agent and methacrylic anhydride. The “octopus-like” surface modification permits to generate so-called *grafting from/to* polymerization process since the covalently anchored active

units (vinyl groups) take part to the free radical polymerization happening in the bulk phase, possessing the active moieties of precursors, both monomers and cross-linkers. The new polymethacrylate monoliths are extensively characterized by a morphological viewpoint by employing a series of advanced techniques including Fourier transform infrared spectroscopy (FT-IR), solid state ^{13}C CPMAS NMR, Scanning Electron Microscopy (SEM) and ^{1}H NMR cryoporosimetry. The kinetic behaviour of these columns for the reversed-phase separation of small molecules and intact proteins is discussed.

2. Experimental

2.1 Chemicals and samples

Fused-silica capillary tubings of 0.250, 0.200 and 0.075 mm I.D. (0.375 mm O.D.) with a polyimide outer coating were purchased from Polymicro Technologies (Phoenix, AZ, USA). Supporting devices to protect the capillary columns were from Avantech Group s.r.l (Angri, SA, Italy). Azoisobutyronitrile (AIBN), acetonitrile (ACN), trifluoroacetic acid (TFA), lauryl methacrylate (LMA), 1,6-hexanediol dimethacrylate (HDDMA), *tert*-butyl alcohol, 1,4-butanediol, tetrahydrofuran (THF), methacrylic anhydride, pyridine, sodium hydroxide (NaOH), hydrochloric acid (HCl), ammonium bicarbonate, uracil, phenol, benzaldehyde, nitro-benzene, benzene, toluene, ethyl-benzene, n-propyl-benzene, n-butyl-benzene, n-pentyl-benzene as well as lysozyme from chicken egg white, α-lactalbumin from bovine milk, β-lactoglobulin B from bovine milk, carbonic anhydrase from bovine erythrocytes, core histones from calf thymus were purchased from Sigma-Aldrich (St. Louis, MO, USA). Porcine trypsin was purchased from Promega (Madison, WI, USA). (N-trimethoxysilylpropyl)-polyethylenimine from United Chemical Technologies (Bristol, PA, USA) was used as a silanization reagent. Plasma protein mixture was solubilized in 25 mM ammonium bicarbonate and subsequently trypsin was added to give an enzyme-to-substrate ratio of 1:50 (w/w). The digest was kept at 37°C overnight, after which the tryptic peptide mixture was

132 acidified with 5% formic acid to terminate the digestion. Desalting and preconcentration of the
133 peptide mixture was performed using a 5-cm long capillary monolithic column (250 μm I.D.).

134 ***2.2 Instrumentation***

135 Diffuse Reflectance Infrared Fourier Transform (DRIFT) and transmission IR (potassium bromide
136 pellets or liquid paraffin dispersion) spectra were recorded on a Jasco 430 Fourier transform (FT)
137 IR spectrometer (Jasco Europe, Cremella, Italy) at a resolution of 4 cm^{-1}.

138 Solid-state ^{13}C CPMAS NMR spectra were carried out at 100.13 MHz on a Bruker Avance III
139 spectrometer. The spin rate was 8000 Hz. The contact time for the cross-polarization was 1 ms, the
140 recycle delay was 3 sec, and the ^{1}H $\pi/2$ pulse was 3.2 μs. The cross-polarization was performed by
141 applying the variable spin-lock sequence RAMP-CPMAS [40], the RAMP was applied on the ^{1}H
142 channel, and during the contact time the amplitude of the RAMP was increased from 50 to 100% of
143 the maximum value. High-power proton dipolar decoupling was carried out using the Spinal-64
144 scheme [41]. The decoupling field was 140 kHz. Spectra were acquired with a time domain of
145 1,024 data points were zero filled and Fourier transformed with 2,048 data points, applying
146 exponential multiplication with 8 Hz line broadening.

147 Scanning Electron Microscopy (SEM) analysis were performed on a FEI Quanta 200 FEG SEM
148 (Eindhoven, The Netherlands) at 30 kV acceleration voltage and with an Everhart-Thornley
149 detector. Before the analysis, samples were mounted onto SEM specimen holders and sputter-
150 coated with a gold-palladium alloy.

151 Wide line ^{1}H NMR spectra of C_6H_6 saturated networks were recorded on a Bruker Avance
152 spectrometer operating at the proton frequency of 300.13 MHz. A variable temperature unit
153 equipped with an N_2 flux from a pressurized line was used in the temperature range 298-190 K.

154 Spectra were recorded by co-adding 32 transients with a recycle delay of 60 sec, the ^{1}H $\pi/2$ pulse
155 was 6 μs. The temperature was carefully calibrated using a 4% methanol in methanol-d_4 standard
156 sample. In the investigated range of temperature, the calibration was carried out recording the
157 chemical shift separation between the OH resonance and the CH_3 resonance of methanol.

^{1}H wide line NMR spectra were deconvoluted using the DM2011 software package. The intensity of NMR signal, the chemical shift, and the width at half-height of C_6H_6 and network resonances were used as input parameters in the deconvolution procedure. The area of the resonance of C_6H_6 obtained from the deconvolution procedure was reported *vs* 1000/T to obtain IT plot.

Chromatographic measurements, under isocratic conditions, were performed on a Waters CapLC system (Waters, Milford, MA, USA) equipped with a home-made injection system consisting in a VICI pneumatic actuator (Valco, Houston, TX, USA) controlled by a home-made electronic time switch, a 2996 ternary CapLC pump and a MicroUVis 20 UV detector (Carlo Erba, Milan, Italy) with an home-made 20 nL perpendicular flow cell. In its optimized configuration, the UV flow cell is characterized by a path length of 150 µm, an illuminated volume of ≈ 20 nL, a connecting tube (150 µm, O.D.) with inner diameter of 30 µm, length of 40 cm and a total volume of 283 nL. Peak variance from peak-width at half-height measured (σ^2) for uracile in ACN/H_2O 60/40 *v/v* was ranging from 130 to 1000 nL^2 at the applied flow rate from 0.5 to 3.0 µL/min; while in the same flow rate regime the second central moment ($\mu'_{2,ex}$) was ranging from 200 to 1300 nL^2 [42]. In all measurements the time constant of 0.10 sec was used. Chromatographic data were collected with a sample rate of 100 Hz and processed using MassLynx 4.1 (Waters, Milford, MA, USA) and Clarity (LabService Analytica, BO, Italy) software. All reported data of plate height, column pressure drop, column permeability and retention were obtained after correction for the system pressure drop and t_0-time measured by removing the column from the system and by a direct connection of a tube (150 µm, O.D.; 30 µm, I.D.; 40 cm, L.) between the pump and the UV cell.

Separations of biomolecules were performed using an UltiMate3000 RSLC nanoLC (Dionex, Amsterdam, NL,USA) equipped with binary separation capillary flow pump, a ternary loading pump, a thermostatted column compartment and a variable wavelength detector with a 7.0 nL Z-shaped flow cell. Time constant and the data collection rate were set to 0.10 sec and 40 Hz

respectively. Chromatographic data were performed with Chromeleon 6.8 (Dionex, Sunnyvale, CA, USA).

MS detection was performed on an Exactive Orbitrap (Thermo Fisher Scientific, San Josè, CA, USA), equipped with a Standard Electrospray Source. The MS instrument was operated at a resolution of 100,000 in positive ESI mode with a sheath gas flow of 15 units, an auxiliary gas of 5 units, a spare gas of 4 units, a spray voltage of 2.3 kV, a capillary voltage of 30 V, a capillary temperature of 275 °C, a tube lens voltage of 240, and a skimmer voltage of 25 V. One microscan was accumulated with a maximum injection time of 100 msec. The MS parameters were optimized in the range of 500-2500 m/z by infusing a solution of 8.0 µM cytochrome C (cat.no C-2506 from Sigma-Aldrich) in H_2O/ACN/TFA (80/20/0.05 *v/v/v*), at resolution of 30,000-100,000 with a syringe pump at a flow rate of 10.00 µL/min.

Mass spectra were collected and processed using Xcalibur software and deconvoluted mass spectra were obtained by using Xtract and ProMass software (Thermo Fisher Scientific).

2.3 Preparation of organic monolithic capillary columns

The monolith was generated by copolymerization of LMA monomer and HDDMA cross-linker as reported in [43], where it was also demonstrated that this stationary phase provides excellent mechanical stability and permeability and very high peak capacity values, making it suitable for separation of intact proteins in miniaturized chromatographic systems.

In the present work, capillary columns were prepared following an innovative multi-step procedure. This consists, firstly, of the pre-treatment of the capillary inner walls as to create a multiple-site tentacle-type activated surface designed to improve the adhesion of the developing polymer to the wall of the inner capillary; then, in the filling of the activated capillaries with the polymerization mixture and, finally, in the irradiation with γ-rays at room temperature (γ-M1) to initiate the polymerization process. For comparative purposes, a thermal monolith (Δ-M2) was also prepared by adding to the same polymerization mixture a free radical initiator (azobisisobutyronitrile) in

amount of 1% w/w with respect to monomers. Polymerization of Δ-M2 was carried out at 50°C for 24 h.

1st step (capillary etching): the inner wall of the fused-silica capillary is treated in a static mode with an aqueous solution of 1 M NaOH for 3 h at 120°C, washed with water, treated with an aqueous solution of 0.1 M HCl for 3 h at 70°C and finally washed with consecutive 5 ml portions of water and methanol and then dried under nitrogen flow.

2nd step (multisite tentacle-type inner wall activation): the pre-treated capillary is filled with a solution of 10% *v/v* (N-trimethoxysilylpropyl)-polyethylenimine in IPA and heated at 70°C for 12 h. After cooling, it is washed with a solution of MeOH/H_2O 60/40 *v/v* containing 10% *v/v* of acetic acid. The filled capillary is then heated at 50°C for 3 h and washed with consecutive 5 ml portions of methanol and THF. By using a syringe, the capillary is filled with a solution of 20% *v/v* of methacrylic anhydride in pyridine/acetonitrile 1/1 *v/v*, heated at 40°C for 2 h, and finally washed with acetonitrile.

3rd step (preparation of the polymerization solution): the polymerization mixture is prepared in a glass vial by admixing monomer, cross-linker and porogens and then degassed by helium sparging for 5 minutes at room temperature. Through a slight argon pressure (ranging from 20 to 60 psi, depending on the diameter and length of the capillary), it is then introduced into the pre-treated capillary in an inert atmosphere. The ends of the capillary columns are finally sealed by silicon rubber.

4th step (polymerization): filled capillaries are placed inside a Gammacell and irradiated at room temperature with a total dose of 40 kGy, with a dose rate of about 2 kGy/h. Instead, for Δ-M2 monolith, filled capillaries are positioned in an oven heated at a temperature of 50°C and maintained for 24 h. Lastly, all capillaries are connected to an apparatus for micro-HPLC and washed with acetone (about 50 column dead volumes) under constant pressure (5 or 10 MPa, depending on the diameter and length of the capillary).

2.4 Chromatographic set-up

In this study, monolithic columns with different internal diameter and length combinations (L. × I.D.) were investigated: 300 and 250 mm × 0.25 mm; 1100 mm × 0.200 mm; 250 mm × 0.075 mm. In order to compare kinetic and thermodynamic performance, we used a homemade packed 5 µm silica Hypersil C18 100 Å capillary column with the same internal diameter and length combinations of both polymethacrylate columns γ-M1 and Δ-M2 (300 × 0.25 mm L. × I.D.). Chromatographic characterization under isocratic elution was carried out in reversed phase mode using ACN/H_2O 60/40 *v/v* as eluent (η= 0.72 cP at 25°C) with a flow rate range extending from 0.250 to 10.00 µL/min at a temperature of 25°C and UV detection at 214 nm. A test mixture of 10 compounds (**1.**uracile, **2.**phenol, **3**.benzaldehyde, **4.**nitrobenzene, **5.**benzene, **6.**toluene, **7.**ethylbenzene, **8.**propylbenzene, **9.**butylbenzene and **10.**pentylbenzene) was used to evaluate the efficiency and retentivity of the columns. van Deemter plots were obtained by fitting the experimental efficiency data (N/m, number of theoretical plates per meter according to European Pharmacopeia, EP) of benzaldehyde as representative analyte for each column. Data fitting of the experimental points to van Deemter equation was performed using Origin 8.0 software and kinetic performance of the different columns were best evaluated using the kinetic plot method [44, 45] setting the maximum backpressure of the HPLC system at 400 bar and the viscosity of the mobile phase at 0.72 cP. Due to the higher chromatographic efficiency of radiolytic monolithic columns (up to 102,000 plate/meter vs. roughly 50,000 plate/m of Δ-M2), capillary-HPLC analysis coupled with high resolution mass spectroscopy (cap-HPLC-HRMS) under RP-gradient conditions were performed by using γ-M1 columns.

3. Results and Discussion

3.1 Conversion efficiency, FT-IR and ^{13}C-CP-MAS NMR investigations

The polymerization mixture, reaction conditions and the monomer/porogen volume ratio affect the morphology of the monoliths in terms of dimension and distribution of pores, and therefore the chromatographic performance of the final columns. In our first experiments (data not shown) we

observed the best kinetic performance when the monomer content in the polymerization mixture was decreased from 40% (high density regime) [28] to 30% (medium density regime). Maintaining the medium density monomers/porogens ratio, γ-M1 monolith was obtained from the optimized polymerization mixture as reported in a previous publication [46].

Quantitative data on monomer conversions were collected using 50 × 10 mm (L. × I.D.) stainless-steel columns filled with the polymerization mixtures and irradiated with a total dose of 40 kGy (γ-M1 column) or alternately heated at 50°C for 24 h (Δ-M2 column).

After completion of the polymerization process, the content of the column was washed *in-situ* using an HPLC pump, dried and removed from the column. Percent conversion, calculated from the known combined weights of monomer and cross-linker introduced into the reaction column, was almost quantitative at total doses of 40 kGy, and close to 98% at 20 kGy. Comparable result (99%) was obtained for thermal triggered polymerization. A total dose of 40 kGy was chosen throughout our study as the best compromise between completeness of the polymerization, acceptable reaction time, and minimum degradation of the formed polymer monolith due to an excessive exposure to γ-radiation. Radiolytic and thermal polymer monoliths also showed superimposable ^{13}C CP-MAS (figure 1) and FT-IR (figure 1-S) spectra, proving either way the achievement of a complete monomer and cross-linker conversion into a saturated polymeric structure. By careful analysis of ^{13}C CPMAS spectra, the peaks of vinyl carbons at about 136 and 125 ppm observed in spectra of monomers are no longer present in the spectrum of the crosslinked monolith (see figure 1). Carbon resonances of methylene (2), methyl (3) and quaternary (1) carbon atoms of the main polymeric backbone are observed at 54.7, 15.2, and 44.0 ppm respectively [47]. The resonance of the carbonyl carbon (4) is observed at 176 ppm. The peak of methylene carbons (5, 10) having an oxygen as first neighbour and belonging to the bridge between polymeric backbones is observed at 63.9 ppm. At the same frequency the peak of methylene carbon (11) having an oxygen as first neighbour and belonging to the side chain is also observed. The peak of terminal methyl (22) is observed at 13.6 ppm, whereas the peak of methylene carbon having the terminal methyl as a first neighbour is

found at 22.3 ppm, and the peak of the methylene carbon having the methyl as a second neighbour is possibly observed at 31.5 ppm. All other methylene carbons (6-9, and 12-19) resonate between 25 and 30 ppm.

FIGURE 1

3.2 Multisite tentacle type inner wall activation

While bulk polymerization of monomers and cross-linkers induced by γ-radiation is straightforward and highly reproducible, polymerization inside HPLC capillaries poses the additional challenge of obtaining a uniform monolith firmly stuck to the inner capillary walls in order to provide a monolithic column. Indeed, any discontinuity of the polymer monolith, causing preferential path flow of the mobile phase, negatively affects the chromatographic performance (wall effect).

In this work, we introduced a new silanization procedure to covalently anchor the monolith to the capillary inner wall surface. After standard etching procedures, the (N-trimethoxysilylpropyl) polyethyleneimine was used as "octopus-like" silanization agent, affording a flexible and multisite reactive surface. The following introduction of unsaturated units with methacrylic anhydride completes the activation of capillary inner walls (figure 2). Then, the polymerization proceeds in a *grafting from/to* fashion, simultaneously from the methacrylate moieties anchored on the polyethyleneimine coating and from methacrylate precursors (monomers and crosslinkers) in the bulk. Thus a monobody polymethacrylate-based column is generated as a highly homogeneous three-dimensional polymeric network firmly anchored to the column inner walls.

FIGURE 2

3.3 Morphological characterization of monoliths

Scanning Electron Microscopy (SEM) yielded valuable structural details on the final polymeric monoliths in the micrometer regime. Morphology of the two different γ-M1 and Δ-M2 polymethacrylate-based monoliths is illustrated by SEM micrographs taken at 800, 10.000 and 30.000 magnifications (figure 3). The composite media reveal the familiar cauliflower internal structure of porous monoliths featuring micro globules of relatively uniform size agglomerated into

larger clusters. Inspection of low magnification SEM micrographs (figure 3, left) reveals that in both cases the monolith was covalently bond to the silica surface and no cracks were present, confirming an effective and efficient *grafting from/to* process.

FIGURE 3

3.4 ^{1}H NMR cryoporosimetry

It has been previously shown that ^{1}H NMR may be used for obtaining the pore size distribution in porous materials with a pore size (Rp) between a few tenths and tens of nanometers [48-53]. Before performing measurements, the porous matrix must be saturated with a liquid probe which must be a non solvent for the porous solid matrix. Then the area of the ^{1}H resonance of the liquid probe must be reported *vs* temperature from room temperature down to low temperature. The obtained IT plot represents the fingerprint of a porous network without requiring any model of the shape of pores [54]. This approach is based on that the freezing temperature of a confined liquid is depressed with respect to the freezing temperature of the bulk liquid [55]. Based on the Gibbs-Thompson equation, the freezing phenomena of a liquid confined into restricted volumes may give information on the pores size distribution. Many porous materials such as zeolites and other silicates have been studied with ^{1}H NMR cryoporosimetry [51]. In these studies, it has been also demonstrated that the pores size distribution obtained by ^{1}H NMR cryoporosimetry compares well with distributions obtained by N_2 adsorption measurements [48]. In particular, with this method the pores structure of water-, benzene-, and cyclohexane-saturated porous silica has been mapped out [48]. We used benzene as a liquid probe to map out the porous structure of our networks.

At room temperature ^{1}H spectra of benzene-saturated networks showed a rather sharp resonance of benzene and a very broad resonance of the solid matrix. By lowering the temperature, the benzene resonance progressively broadened and decreased in intensity. ^{1}H spectra were deconvoluted to obtain the area of both resonances. According to the IT method, the integral of the benzene resonance was reported *vs* 1000/T. IT plots of sample γ-M1 (a) and Δ-M2 (b) are shown in figure 4.

Note that the steep transition of signal intensity observed in both samples between 283 and 278 K was due to the freezing of bulk C_6H_6. At lower temperatures, sample γ-M1 showed just one intensity transition whereas sample Δ-M2 showed two transitions. These intensity transitions are due to freezing of benzene confined in pores with a different average dimension. In figure 4 these transitions are evidenced with arrows.

The intensity of a liquid probe confined in a porous matrix is related to X=1000/T through the equation [5]:

$$I(X) = \sum_{i=1}^{N} \frac{I_{0i}}{2}\left[1 + \mathrm{erf}\left[\frac{X_{ci} - X}{\Delta_i \sqrt{2}}\right]\right] \quad (1)$$

where I0i, Xci and Δi represent the intensity, the inverse transition temperature (Xci=1000/Tci) and the width of the temperature distribution curve of phase i, I(X) represents the total amount of the liquid probe confined in pores at the inverse temperature X=1000/T and N is the number of temperature transitions. Note that, for a very sharp transition Δi tends to 0, while the broader the transition the higher the Δi value. Parameters I_{0i}, X_{ci} and Δi were obtained fitting the experimental data to equation 1, see table 1, the uncertainty on data reported in the table varies between 6 and 10%.

According to the literature [48], differentiating equation 1 with respect to X and using an equation which correlates the freezing point temperature depression ΔT of the confined liquid to the pore radius (Rp) it is possible to obtain the pore size distribution:

$$\frac{dI}{dRp} = \sum_{i=1}^{N} \frac{I_{0i}}{1000 K_b \Delta_i \sqrt{2\pi}} \left(XT_0 - 1000\right)^2 \exp\left[-\left(\frac{X - X_{ci}}{\Delta\sqrt{2}}\right)^2\right] \quad (2)$$

where T_0= 278.5 K is the freezing temperature of bulk benzene, and K_b= 1107 K was obtained from literature data [48].

Using equation 2 and the parameters reported in table 1, the pore size distributions for samples γ-M1 and Δ-M2 was obtained (see figure 4C).

It is worth noticing that sample γ-M1 showed one asymmetric distribution centered at about 13 nm, whereas sample Δ-M2 showed a bimodal distribution with a sharp peak centered at about 2.5 and a broad asymmetric peak centered at about 8 nm in a relative amount of 36 and 64%.

Table 1

FIGURE 4

3.5 Permeability and Efficiency

The plot of the backpressure generated by the column (ΔP_c) against the mobile phase linear velocity (μ_0) is reported on the left side of figure 5 for two monolithic columns (300 mm × 250 µm, L × I.D.) and a Hypersil C18 packed column (particle size 5 µm, 300 mm × 0.250 mm, L × I.D.). Linear velocities are calculated through the elution time, t_0, of an unretained/unexcluded compound ($\mu_0 = L/t_0$). The linear dependence of ΔP_c on μ_0 (linear regression R^2s > 0.999) show that the monolithic bed is stable without suffering compression. From these plots, column permeability K_0 [56] can be calculated according to:

$$K_0 = \frac{\mu_0 \eta L}{\Delta P_c} \quad (1)$$

where η is the viscosity of the solvent and L the column length. Alternatively, the specific permeability K_{SF} is given by:

$$K_{SF} = \frac{\eta L \Phi}{r^2 \pi \Delta P_c} \quad (2)$$

where Φ is the flow rate and r the radius of column. Both the permeability and the specific permeability values obtained by linear regression analysis of ΔP *vs* μ_0 (or ΔP *vs* Φ) plots are summarized in table 2.

FIGURE 5

The maximum pressure drop recorded at the highest linear velocity was around 2200 and 830 psi for γ-M1 and Δ-M2 monolith columns respectively, while a value of 2500 psi was found for the packed column.

The total porosity of monolithic columns can be calculated as:

$$\varepsilon_T = K_{SF}/K_0 \quad (3)$$

Total porosities of monolothic columns were very similar each other and significantly higher than that of the packed particle column. On the other hand, the larger permeability of Δ-M2 (K_0 = 18.0) with respect to γ-M1 (K_0 = 7.0) is probably due to the presence of a lesser dense organization of microglobules, which demonstrates how polymerization procedure (radiolitic or thermic) has a noteworthy impact on the dimensions of throughpores. In order to compare hydrodynamic properties of monolithic and packed columns, permeability-equivalent particle diameter d_{perm} [58] was calculated using the following equation:

$$d_{perm} = \sqrt{1000 \times K_{SF}} \quad (4)$$

where 1000 is the so-called flow resistance value for a typical packed column with external porosity of about 0.4. Thus the permeability of γ-M1 monolith is comparable to that of a column packed with spherical particles of about 7 µm diameter, while the permeability of Δ-M2 is higher and comparable to that of a column packed with 11.5 µm particles (table 2).

Table 2

To evaluate the kinetic performance of both monolithic and packed columns, the traditional efficiency-linear velocity plots were built using benzaldehyde as retained solute (figure 5, right) in ACN/H_2O 60/40 *v/v* at 25°C, by changing the eluent linear velocity from 0.12 to maximum 5.00 mm/s. The data were therefore fitted to the van Deemter equation:

$$H = \mathrm{A} + \frac{B}{\mu_0} + C \times \mu_0 \quad (5)$$

and the best numerical values of the fitted coefficients *A*, *B* and *C* are reported in table 2.

The minima of the van Deemter curves for the monolithic columns were H_{min} = 9.8 and 18.9 µm for γ-M1 and Δ-M2 respectively; on the other hand, the packed column exhibited H_{min} of 12.9 µm. Observation of figure 5 shows that the van Deemter curve of γ-M1 monolithic column is characterized by a less steep C branch portion due to a lower mass transfer resistance in the porous

structure. It is thus more suitable for high velocity and high efficient separations. The almost twice larger C-term of Δ-M2 column compared to that of γ-M1 one, despite the fact that the two monoliths have identical chemistry, points out that the radiolitic polymerization procedure favours the achievement of a more microglobular structure (figure 4). γ-M1 monolith showed higher flow-resistance than Δ-M2 thermal monolith and enhanced kinetic behavior (lower *C* and H_{min} values) even compared with the Hypersil C18 column packed with 5 μm particles. An extended van Deemter ispection of the behavior of these two columns is reported under Supporting Information (figure S2) where van Deemter curves for a series of low molecular weight compounds with capacity factor included between 0.30-7.0 (γ-M1 monolith) and 0.7-8.8 (Hypersil C18, 5 μm column) are presented. Remarkably, efficiency of about 100,000 plate/meter was observed also using 75 μm I.D. monolithic column, which represents a considerable result in the practice of miniaturized nano liquid chromatography (figure S3).

3.6 Reproducibility and long-term stability

Run-to-run and batch-to-batch reproducibility of γ-M1 monolith were assessed by performing a series of injections of a sample of four standard proteins in gradient elution mode. The comparison of retention time of the test compounds in a series of five consecutive injections were characterized by a relative standard deviation (RSD) smaller than 1% for each component (figure S4-A) showing therefore a very high run-to-run reproducibility. Analogous results (RSD <1%) were obtained also in terms of batch-to-batch reproducibility, as detailedly described under Supporting Information (figure S4-B). Finally, the long term column stability was also investigated by considering the separation of the same mixtures of core histones from calf thymus on a new monolithic column and on the same column after 1000 runs (see Supporting Information, figure S4-C): even in this case, the RSD of retention times of corresponding peaks was about 1.%.

3.7 Kinetic Plots

The Kinetic Plot Method (KPM) is a powerful tool to predict the theoretical highest performance achievable in the shortest possible time at the maximum pressure allowed by the system [44,45].

KPM is useful not only to evaluate column quality but also to compare the kinetic performance of columns with different size and morphology. In this study, kinetic plots were calculated by assuming 6000 psi as the maximum HPLC backpressure and 0.72 cP as the mobile phase viscosity. Specific permeabilities, as well as values of μ_0 and H were obtained experimentally (see before). The resulting t_0/N *vs.* N (so-called Poppe plot) and t_0/N^2 *vs.* N plots are shown in figure 6A and B respectively. Poppe plot [59] (figure 6A) reflects the separation speed that can be achieved at the maximum pressure. Fastest separations are located in the bottom left corner, while analysis with high resolution and efficiency are in the top-right of the plot. Given the comparable C-terms of γ-M1 and C18 silica-based columns, significantly lower than that Δ-M2 monolith (see table 2), they both allow to achieve very large efficiency in shorter times than for the thermal monolith. Since, the higher permeability of monolithic columns allows using longer columns at a fixed maximum pressure and higher plate numbers can be achieved only with monoliths. For lower N values, essentially the same length of γ-M1 and Hypersil C18 columns is required, while the Δ-M2 would need to be twice as long. Figure 6B shows impedance time t_0/N^2 *vs.* N plots. In these plots, N-values (*x*-axis) are in reversed order with respect to Poppe plot, so that they visually resemble to traditional van Deemter plots. For the Hypersil C18, 5 µm column the minimum corresponds to N = 300,000 plates with L= 4 m, while the γ-M1 and Δ-M2 columns show N values two and three times higher, with L= 6.6 and 19 m respectively. Although these are only theoretical calculations not practicable for most HPLC applications, especially for silica-packed columns, the KPM can be used to predict and produce very long monolithic columns with a high permeability, reaching efficiency values of well over 100 000 theoretical plates.

FIGURE 6

3.8 Thermodynamic investigation: retention and methylene selectivity

Hydrophobicity of the columns was investigated through the retention behavior of a series of small molecules (phenol, benzaldehyde, nitrobenzene, benzene, toluene, ethylbenzene, propylbenzene, butylbenzene and pentylbenzene) in reversed phase mode (using ACN/H_2O, 60/40 *v/v*). Figure 7

compares the chromatograms obtained with the three columns. First of all, one may notice the different behavior in terms of retention between the two monolithic columns. As detailedly reported under Supporting Information (table S1)**,** retention factors *(k*s*)* measured on the Δ-M2 monolith were systematically larger than those of the radiolitic column (figure 4C).

The homologous series of alkylbenzenes (from benzene to pentylbenzene) can be used to estimate the methylene selectivity (α_{CH2}) of the stationary phase, i.e. its ability to distinguish between two compounds differing by a single methylene group [60-62]. In figure S5, the plots of the logarithmic of retention factor *vs.* the incremental number of methylene groups are reported. This study evidenced that the two monolithic columns have essentially the same α_{CH2} (log*k vs* n_{CH2} plots having the same slope). On the other hand, the γ-M1 column showed a remarkably lower value of the y-intercept compared to that of the Δ-M2, which reflects a lower contribution by the aromatic end group to retention.

FIGURE 7

3.9 Capillary LC-MS top-down proteomic analysis

Due to its high efficiency and permeability, γ-M1 monolithic capillary column was tested for the separation intact proteins. In fact, its low flow resistance allowed to reach significantly large flow rates (in the order of 15 µL/min) suitable for coupling the column to MS detector through standard electrospray interface (ESI).

A standard mixture of four intact proteins was analyzed on the γ-M1 column (250 × 0.250 mm L. × I.D.) using gradient elution and high resolution MS detection (figure 8). As it can be seen from the figure, total ion current chromatogram showed additional peaks (with respect to UV signal). The assignement of each peak was obtained by deconvolution of multicharged MS spectra as reported under Supporting Information (figure S6). Briefly, two different lyzozyme isoforms (**p1-a**, **p1-b**) and two impurities of carbonic anhydrase (**i-1**, **i-2**) could be identified (see table S2 of Supporting Information). Signals due to multiply charged ions (z always higher than +13) were recorded with high isotopic resolution (about 40-50,000) for all proteins except than **p4**. The exact mass of **p4**

(29022.8 Da) was determined by artifact-free deconvolution of low z multicharged signals using ProMass. The separation of real complex peptide sample was also performed by using a very long column (110 cm × 200 μm, L × I.D.) directly interfaced to the mass spectrometer via standard ESI source. Maintaining the column pressure at an acceptable level, plasma proteins digest was well separated with a 50 min gradient at 7 μL/min flow rate.

FIGURE 8

FIGURE 9

4. Conclusions

Gamma radiation offers an alternative route for an easy *in-situ* preparation of macroporous polymeric monoliths suitable as separation media in analytical chemistry. In this work, to obtain the capillary column, an innovative "tentacle type" *grafting from/to* approach producing multisite, flexible grafted reactive surface of capillary inner walls was proposed. Monolithic stationary phases for capillary HPLC characterized by chromatographic efficiencies > 102,000 plate/m were prepared under continuous γ-ray exposure. The chemical, physical and morphological properties of lauryl methacrylate-1,6-hexanediol dimethacrylate co-polymer were investigated by FT-IR, solid state ^{13}C CPMAS NMR, SEM and ^{1}H NMR cryoporosimetry. The evaluation of chromatographic performance, using a set of small molecules, has revealed high efficiency and resolution power, together with low flow resistance and significant mechanical stability. Moreover, the fabricated columns demonstrated excellent reproducibility with RSD values for run-to-run and column-to-column below 1%. Efficient separation of intact proteins and peptides by LC-MS on lauryl polymethacrylate-based monolithic capillary columns was realized, demonstrating their potential use in top-down and bottom-up proteomic studies.

Acknowledgments

This study was supported by PRIN contract n. 2012ATMNJ_003 and by Sapienza Università di Roma contract n. C26H13ZSR4. The authors thank Mr. Enrico Rossi as technical assistant in NMR

measurements. The authors are also grateful to Avantech group s.r.l (Angri, SA, Italy) for the supporting devices of capillary columns.

The authors have declared no conflict of interest.

5. References

[1] P. A. Levkin, S. Eeltink, T.R. Stratton, R. Brennen, K. Robotti, H. Yin, K. Killeen, F. Svec, J. M. Fréchet, Monolithic porous polymer stationary phases in polyimide chips for the fast high-performance liquid chromatography separation of proteins and peptides, J. Chromatogr. A 1200 (2008) 55-61.

[2] F. Svec, Less common applications of monoliths: Preconcentration and solid-phase extraction, J. Chromatogr. B 841 (2006) 52-64.

[3] Y. Hu, Y. Fan, G. Li, Preparation and evaluation of a porous monolithic capillary column for microextraction of estrogens from urine and milk samples online coupled to high-performance liquid chromatography, J. Chromatogr. A 1228 (2012) 205-2012.

[4] A. Nordborg, E.F. Hilder, Recent advances in polymer monoliths for ion-exchange chromatography, Anal. Bioanal. Chem. 394 (2009) 71-84.

[5] G. Zhu, L. Zhang, H. Yuan, Z. Liang, W. Zhang, Y. Zhang, Recent development of monolithic materials as matrices in microcolumn separation systems, J. Sep. Sci. 30 (2007) 792-803.

[6] J. Urban, P. Jandera, Polymethacrylate monolithic columns for capillary liquid chromatography, J. Sep. Sci. 31 (2008) 2521-2540.

[7] R. Wu, L. Hu, F. Wang, M. Ye, H. Zou, Recent development of monolithic stationary phases with emphasis on microscale chromatographic separation, J. Chromatogr. A 1184 (2008) 369-392.

[8] G. Guiochon, Monolithic columns in high-performance liquid chromatography, J. Chromatogr. A 1168 (2007) 101-168.

[9] K.K. Unger, R. Skudas, M.M. Schulte, Particle packed columns and monolithic columns in high-performance liquid chromatography-comparison and critical appraisal, J. Chromatogr. A 1184 (2008) 393-415.

[10] F. Svec Y. Lv, Advances and Recent Trends in the Field of Monolithic Columns for Chromatography, Anal. Chem. 87 (2015) 250-273.

[11] H. Minakuchi, K. Nakanishi, N. Soga, N. Ishizuka, N. Tanaka, Octadecylsilylated porous silica rods as separation media for reversed-phase liquid chromatography, Anal. Chem. 68 (1996) 3498-3501.

[12] R.D. Arrua, M. Talebi, T.J. Causon, E.F. Hilder, Review of recent advances in the preparation of organic polymer monoliths for liquid chromatography of large molecules, Anal. Chim. Acta 738 (2012) 738 1-12.

[13] E.C. Peters, M. Petro, F. Svec, J. M. Fréchet, Molded rigid polymer monoliths as separation media for capillary electrochromatography. 2. Effect of chromatographic conditions on the separation, Anal. Chem. 70 (1998) 2296-2302.

[14] X. Huang, S. Zhang, G.A. Schultz, J. Henion, Surface-alkylated polystyrene monolithic columns for peptide analysis in capillary liquid chromatography-electrospray ionization mass spectrometry, Anal. Chem. 74 (2002) 2336-2344.

[15] R. Shediac, S.M. Ngola, D.J. Throckmorton, D.S. Anex, T.J. Shepodd, A.K. Singh, Reversed-phase electrochromatography of amino acids and peptides using porous polymer monoliths, J. Chromatogr. A 925 (2001) 251-263.

[16] A. Premstaller, H. Oberacher, W. Walcher, A.M. Timperio, M. Zolla, J.P. Chervet, N. Cavusoglu, N. van Dorsselaer, C. Huber, High-performance liquid chromatography-electrospray ionization mass spectrometry using monolithic capillary columns for proteomic studies, Anal. Chem. 73 (2001) 2390-2396.

[17] A. Vellaichamy, J.C. Tran, A. D. Catherman, J.E. Lee, J.F. Kellie, S.M.M. Sweet, L. Zamdborg, P.M. Thomas, D.R. Ahlf, K.R. Durbin, G.A. Valaskovic, N.L. Kelleher, Size-sorting

563 combined with improved nanocapillary liquid chromatography-mass spectrometry for identification
564 of intact proteins up to 80 kDa, Anal. Chem. 82 (2010) 1234-1244.
565 [18] I. Nischang, Porous polymer monoliths: morphology, porous properties, polymer nanoscale gel
566 structure and their impact on chromatographic performance, J. Chromatogr. A 1287 (2013) 39-58.
567 [19] Y. Shen, L. Qi, Mao L., Macroporous polymer monoliths with a well-defined three
568 dimensional skeletal morphology derived from a novel phase separator for HPLC, Polymer 53
569 (2012) 4128-4134.
570 [20] J. Urban, P. Jandera, P. Langmaier, Effects of functional monomers on retention behavior of
571 small and large molecules in monolithic capillary columns at isocratic and gradient conditions, J.
572 Sep. Sci. 34 (2011) 2054-2062.
573 [21] A. Nordborg, F. Svec, J.M. Fréchet, K. Irgum, Extending the array of crosslinkers suitable for
574 the preparation of polymethacrylate-based monoliths, J. Sep. Sci. 28 (2005) 2401-2406.
575 [22] S.H. Lubbad, M.R. Buchmeiser, Highly cross-linked polymeric capillary monoliths for the
576 separation of low, medium, and high molecular weight analytes, J. Sep. Sci. 32 (2009) 2521-2529.
577 [23] P. Jandera, M. Staňkova, V. Škeřikova, J. Urban, Cross-linker effects on the separation
578 efficiency on (poly)methacrylate capillary monolithic columns. Part I. Reversed-phase liquid
579 chromatography, J. Chromatogr. A 1274 (2013) 97-106.
580 [24] C. P. Bisjak, S. H. Lubbad, L. Trojer, G. K. Bonn, Novel monolithic poly(phenyl acrylate-co-
581 1,4-phenylene diacrylate) capillary columns for biopolymer chromatography, J. Chromatogr. A
582 1147 (2007) 46-52.
583 [25] C. P. Bisjak, L. Trojer, S.H. Lubbad, W. Wieder, G.K. Bonn, Influence of different
584 polymerisation parameters on the separation efficiency of monolithic poly(phenyl acrylate-co-1,4-
585 phenylene diacrylate) capillary columns, J. Chromatogr. A 1154 (2007) 269-276.
586 [26] A. Greiderer, L. Trojer, C. W. Huck, G. K. Bonn, Influence of the polymerisation time on the
587 porous and chromatographic properties of monolithic poly(1,2-bis(p-vinylphenyl))ethane capillary
588 columns, J. Chromatogr. A 1216 (2009) 7747-7754.

589 [27] L. Trojer, C. P. Bisjak, W. Wieder, G. K. Bonn, High capacity organic monoliths for the
590 simultaneous application to biopolymer chromatography and the separation of small molecules, J.
591 Chromatogr. A 1216 (2009) 6303-6309.
592 [28] S. Eeltink, J.M. Herrero-Martinez, G.P. Rozing, P. J. Schoenmakers, W.T. Kok, Tailoring the
593 morphology of methacrylate ester-based monoliths for optimum efficiency in liquid
594 chromatography, Anal. Chem. 77 (2005) 7342-7347.
595 [29] P. Aggarwal, J. S. Lawson, H. D. Tolley, M. L. Lee, High efficiency polyethylene glycol
596 diacrylate monoliths for reversed-phase capillary liquid chromatography of small molecules, J.
597 Chromatogr. A 1364 (2014) 96-106.
598 [30] B. Singco, C. L. Lin, Y. J. Cheng, Y. H. Shih, H. Y. Huang, Ionic liquids as porogens in the
599 microwave-assisted synthesis of methacrylate monoliths for chromatographic application, Anal.
600 Chim. Acta 746 (2012) 123-133.
601 [31] F. Svec, Porous polymer monoliths: amazingly wide variety of techniques enabling their
602 preparation, J. Chromatogr. A 1217 (2010) 902-924.
603 [32] Á. Sáfrány, B. Beiler, K. László, F. Svec, Control of pore formation in macroporous polymers
604 synthesized by single-step γ-radiation-initiated polymerization and cross-linking, Polymer 46
605 (2005) 2862-2871.
606 [33] B. Beiler, Á Vincze, F. Svec, Á. Sáfrány, Poly(2-hydroxyethyl acrylate-co-ethyleneglycol
607 dimethacrylate) monoliths synthesized by radiation polymerization in a mold, Polymer 48 (2007)
608 3033-3040.
609 [34] J. Courtois, M. Szumski, E. Byström, A. Iwasiewicz, A. Shchukarev, K. Irgum, A study of
610 surface modification and anchoring techniques used in the preparation of monolithic microcolumns
611 in fused silica capillaries, J. Sep. Sci. 29 (2006) 14-24.
612 [35] G.T.T. Gibson, S. M. Mugo, R.D. Oleschuk, Surface-mediated effects on porous polymer
613 monolith formation within capillaries, Polymer 49 (2008) 3084-3090.

614 [36] J. Vidič, A. Podgornik, A. Štrancar, Effect of the glass surface modification on the strength of
615 methacrylate monolith attachment, J. Chromatogr. A 1065 (2005) 51-58.
616 [37] B. Zhao, W.J. Brittain, Polymer Brushes: Surface-Immobilized Macromolecules, Prog. Polym.
617 Sci. 25 (2000) 677-710.
618 [38] R. Barbey, L. Lavanant, D. Paripovic, N. Schüwer, C. Sugnaux, S. Tugulu, H.A. Klok,
619 Polymer brushes via surface-initiated controlled radical polymerization: synthesis, characterization,
620 properties, and applications, Chem. Rev. 109 (2009) 5437-5527.
621 [39] S. Minko, S. Patil, V. Datsyuk, F. Simon, K. J. Eichhorn, M. Motornov, D. Usov, I. Tokarev,
622 M. Stamm, Synthesis of Adaptive Polymer Brushes via "Grafting To" Approach from Melt,
623 Langmuir 18 (2002) 289-296.
624 [40] G. Metz, X. Wu, S. O. Smith, Ramped-amplitude cross polarization in magic-angle-spinning
625 NMR, J. Magn. Reson. A 110 (1994) 219-227.
626 [41] G. Comellas, J.J. Lopez, A.J. Nieuwkoop, L.R. Lemkau, C.M. Rienstra, Straightforward,
627 effective calibration of SPINAL-64 decoupling results in the enhancement of sensitivity and
628 resolution of biomolecular solid-state NMR, J. Magn. Reson. 209 (2011) 131-135.
629 [42] F. Gritti, G. Guiochon, On the extra-column band-broadening contributions of modern, very
630 high pressure liquid chromatographs using 2.1 mm I.D. columns packed with sub-2 μm particles, J.
631 Chromatogr. A 1217 (2010) 7677-7689.
632 [43] P. Simone, G. Pierri, P. Foglia, F. Gasparrini, G. Mazzoccanti, A.L. Capriotti, O. Ursini, A.
633 Ciogli, A. Laganà, Separation of intact proteins on γ-ray-induced polymethacrylate monolithic
634 columns: A highly permeable stationary phase with high peak capacity for capillary high-
635 performance liquid chromatography with high-resolution mass spectrometry, J. Sep. Sci. 39 (2016)
636 264–271.
637 [44] G. Desmet, D. Clicq, P. Gzil, Geometry-independent plate height representation methods for
638 the direct comparison of the kinetic performance of LC supports with a different size or
639 morphology, Anal. Chem. 77 (2005) 4058-4070.

640 [45] D. Kotoni, A. Ciogli, C. Molinaro, I. D'Acquarica, J. Kocergin, T. Szczerba, H. Ritchie, C.
641 Villani, F. Gasparrini, Anal. Chem. 84 (2012) 6805-6813.
642 [46] G. Pierri, D. Kotoni, P. Simone, C. Villani, G. Pepe, P. Campiglia, P. Dugo, F. Gasparrini,
643 Analysis of bovine milk caseins on organic monolithic columns: an integrated capillary liquid
644 chromatography-high resolution mass spectrometry approach for the study of time-dependent
645 casein degradation, J. Chromatogr. A 1313 (2013) 259-269.
646 [47] F.A. Bovey, P.A. Mirau, NMR of Polymers, Academic Press, San Diego, California, 1996.
647 [48] E. W. Hansen, R. Schimdt, M. Stöcker, Pore Structure Characterization of Porous Silica by 1H
648 NMR Using Water, Benzene, and Cyclohexane as Probe Molecules, J. Phys. Chem. 100 (1996)
649 11396-11401.
650 [49] K. Overloop, L. Van Gerven, Freezing Phenomena in Adsorbed Water as Studied by NMR, J.
651 Magn. Reson. A101 (1993) 179-187.
652 [50] R. Schmidt, E.W. Hansen, M. Stöcker, D. Akporiaye, O.H. Ellestad, Water-Saturated
653 Mesoporous MCM-41 Systems Characterized by 1H NMR Spin-Lattice Relaxation Times, J. Phys.
654 Chem. 99 (1995) 4148-4154.
655 [51] D. Akporiaye, E.W. Hansen, R. Schmidt, M. Stöcker, Water-Saturated Mesoporous MCM-41
656 Systems Characterized by 1H NMR, J. Phys. Chem. 18 (1994) 1926-1928.
657 [52] E.W. Hansen, R. Schmidt, M. Stöcker, D. Akporiaye, Water-Saturated Mesoporous MCM-41
658 Systems Characterized by 1H NMR Spin-Lattice Relaxation Times, J. Phys. Chem. 99 (1995)
659 4148-4154.
660 [53] E.W. Hansen, M. Stöcker, R. Schmidt, Low-Temperature Phase Transition of Water Confined
661 in Mesopores Probed by NMR. Influence on Pore Size Distribution, J. Phys. Chem. 100 (1996)
662 2195-2200.
663 [54] D. Capitani, N. Proietti, F. Ziarelli, A.L. Segre, NMR Study of Water-Filled Pores in One of
664 the Most Widely Used Polymeric Material: The Paper, Macromolecules 35 (2002) 5536-5543.

665 [55] J.H. Strange, M. Rahman, E.G. Smith, Characterization of porous solids by NMR, Phys. Rev.
666 Lett. 71 (1993) 3589-3591.
667 [56] J. Grafnetter, P. Coufal, E. Tesarovà, J. Suchànkovà, Z. Bosakova, J. Sevcìk, Optimization of
668 binary porogen solvent composition for preparation of butyl methacrylate monoliths in capillary
669 liquid chromatography, J. Chromatogr. A 1049 (2004) 43-49.
670 [57] K. R. Harris, Temperature and density dependence of the self-diffusion coefficient of n-hexane
671 from 223 to 333 K and up to 400 MPa, Journal Chem. Soc., Faraday Trans. 1 78 (1982) 2265-2274.
672 [58] S. Eeltink, P. Gzil, W. T. Kok, P.J. Schoenmakers, G. Desmet, Selection of comparison criteria
673 and experimental conditions to evaluate the kinetic performance of monolithic and packed-bed
674 columns, J. Chromatogr. A 1130 (2006) 108-114.
675 [59] H. Poppe, Some reflections on speed and efficiency of modern chromatographic methods, J.
676 Chromatogr. A 778 (1997) 3-21.
677 [60] J. Layne, Characterization and comparison of the chromatographic performance of
678 conventional, polar-embedded, and polar-endcapped reversed-phase liquid chromatography
679 stationary phases, J. Chromatogr. A 957 (2002) 149–164.
680 [61] N. Marchetti, L. Caciolli, A. Laganà, F. Gasparrini, L. Pasti, F. Dondi, A. Cavazzini, Fluorous
681 affinity chromatography for enrichment and determination of perfluoroalkyl substances, Anal.
682 Chem. 84 (2012) 7138–7145.
683 [62] M. Catani, R. Guzzinati, N. Marchetti, L. Pasti, A. Cavazzini, Exploring Fluorous Affinity by
684 Liquid Chromatography, Anal. Chem. 87 (2015) 6854–6860.
685
686
687
688
689
690

691 **Figure captions**

692 **Figure 1.** Solid state ^{13}C CPMAS NMR spectra of thermal (a) and radiolytic (b) monoliths.
693 Assignement was discussed in the text.

694 **Figure 2.** Tentacle type inner wall activation and *grafting on-to* polymerization process.

695 **Figure 3.** SEM images of γ-M1 (top) and Δ-M2 (bottom) monoliths**.**

696 **Figure 4.** IT plots of sample γ-M1 (a) and Δ-M2 (b), solid lines through the experimental points
697 were obtained fitting the experimental data to equation 1. Pore size distribution of samples γ-M1
698 and Δ-M2 obtained from equation 2.

699 **Figure 5.** Pressure-linear flow velocity plots (left) and van Deemter plots (right) for columns
700 containing ◒ γ-M1_300 mm × 0.25 mm monolith and ○ Δ-M2_300 mm × 0.25 mm monolith in
701 comparison to ● Hypersil C18, 5 µm packed column (300 mm × 0.25 mm L. × I.D.). Eluent:
702 ACN/H_2O 60/40 *v/v*, viscosity given as η = 0.72 cP at 25 °C. Uracil for permeability data, and
703 benzaldehyde (*k*: 0.30 for γ-M1; *k*: 0.38 for Δ-M2 and *k*: 0.72 for Hypersil C18, 5 µm) for van
704 Deemter inspection, were used as markers.

705 **Figure 6.** Poppe plot (top) and t_0/N^2 *vs.* N (bottom) for ethylbenzene. Columns: (◉) γ-M1_300 mm
706 × 0.25 mm monolith, (●) Δ-M2_300 mm × 0.25 mm monolith and (●) Hypersil C18, 5 µm 300 mm
707 × 0.25 mm**.** Mobile phase: ACN/H_2O 60/40, *v/v*; T_{col}: 25 °C. Maximum system pressure: 6000 psi.

708 **Figure 7.** Comparison of isocratic elution on γ-M1_300 mm × 0.25 mm (top), Hypersil C18, 5 µm
709 300 mm × 0.25 mm (middle) and Δ-M2_300 mm × 0.25 mm (bottom) by eluting a small molecules
710 mixture. Mobile phase: ACN/H_2O 60/40 *v/v*; detection wavelength: 214 nm; flow rate: 1.0 µl/min.
711 Results are expressed as theoretical plates per meter (N/m).

712 **Figure 8.** Total ion current chromatogram and UV traces of standard proteins mixture (**i-1** and **i-2.**
713 impurity **1** and **2** of the carbonic anhydrase, respectively, **p1-a**. lysozyme isoform a, **p1-b.** lysozyme
714 isoform b, **p2**. α-lactalbumin, **p3**. β-lactoglobulin, **p4**. carbonic anhydrase) on γ-M1_250 mm ×
715 0.25 mm monolith. Mobile phases: (A) H_2O/ACN 95/5 + 0.1% TFA; (B) ACN/H_2O 95/5 + 0.1%

716 TFA; 15 min gradient elution from 5% to 70% of mobile phase B; flow rate: 15 μL/min; T_{col}: 60
717 °C.
718 **Figure 9.** Total ion current chromatogram of plasma protein digest (CapHPLC-HRMS analysis).
719 Pre-Column: γ-M1 5 cm × 0.25 mm L. × I.D. Loading solvent: 0.1% aqueous trifluoroacetic acid;
720 trapping time: 5 min; loading flow rate: 10 μL/min; Column: γ-M1_1100 mm × 0.200 mm L. × I.D.
721 Mobile phases: (A) H_2O/ACN 95/5 + 0.1% TFA; (B) ACN/H_2O 95/5 + 0.1% TFA; gradient elution
722 from 3% to 35% of mobile phase B in 40 min, from 35% to 50% in 1 min, from 50% to 70% in 4
723 min and finally hold for 5 min; flow rate: 7 μL/min; T_{col}: 60 °C.
724
725
726
727
728
729
730
731
732
733
734
735
736
737

Figure

Click here to download high resolution image

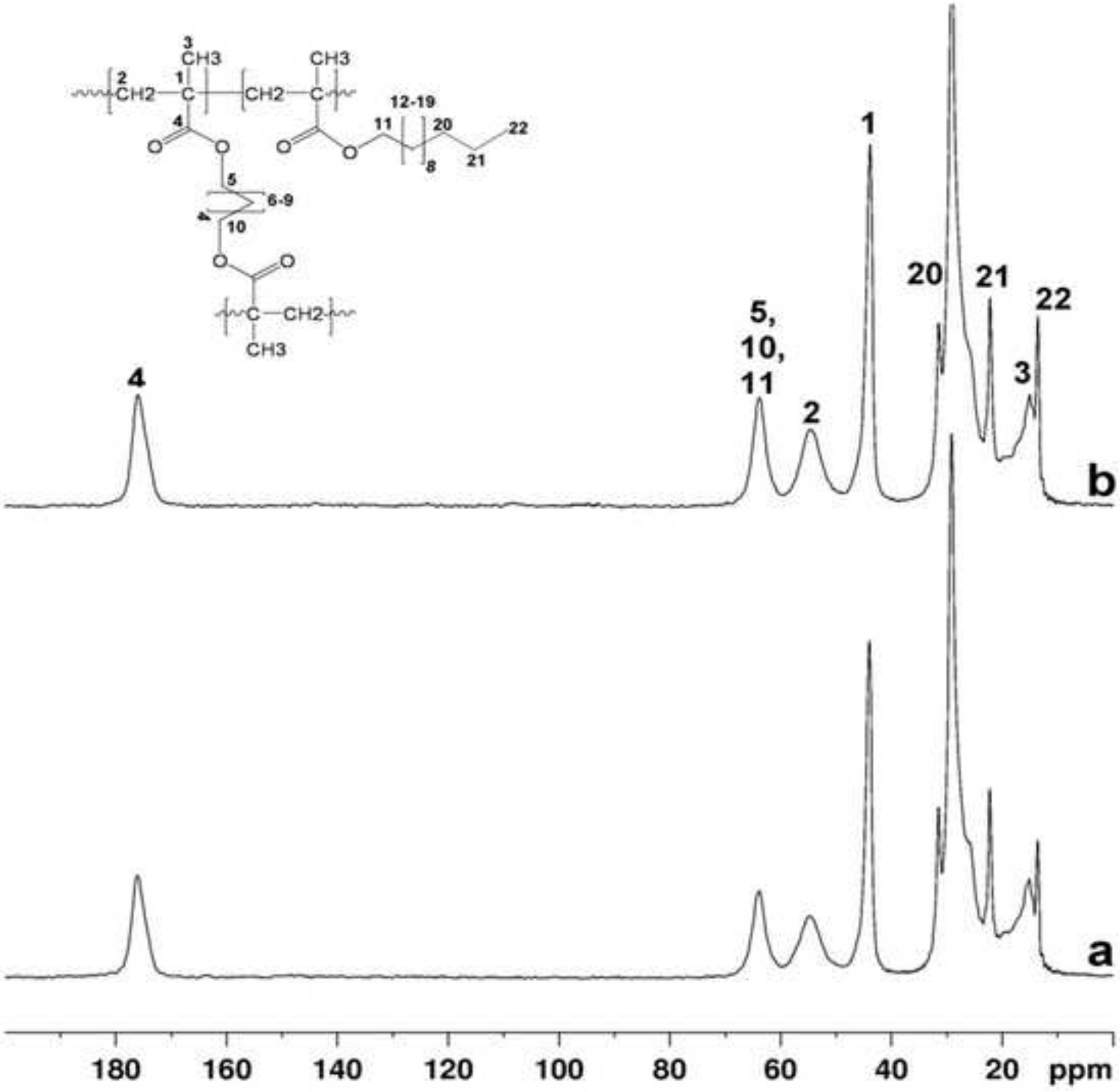

Figure

Click here to download high resolution image

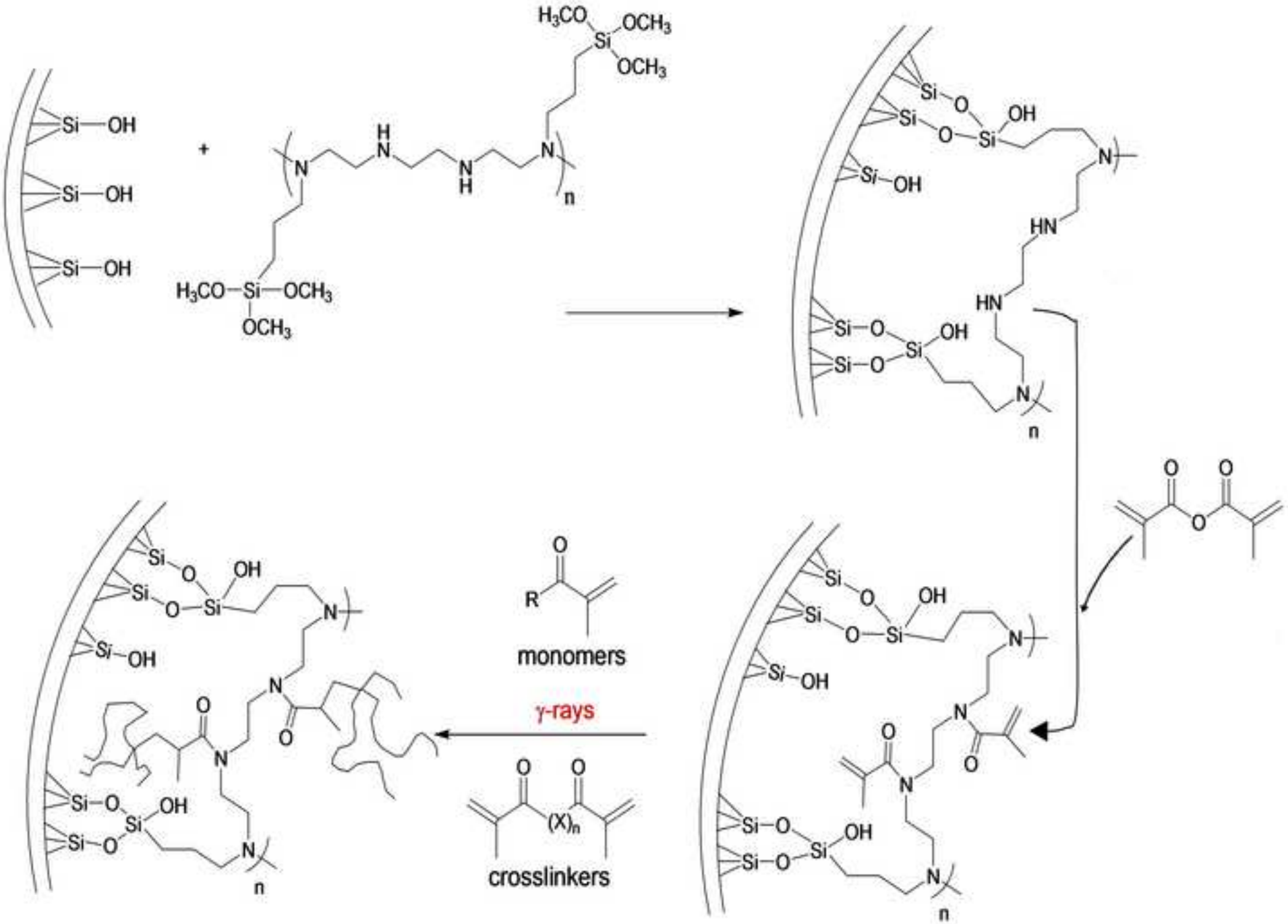

Figure

Click here to download high resolution image

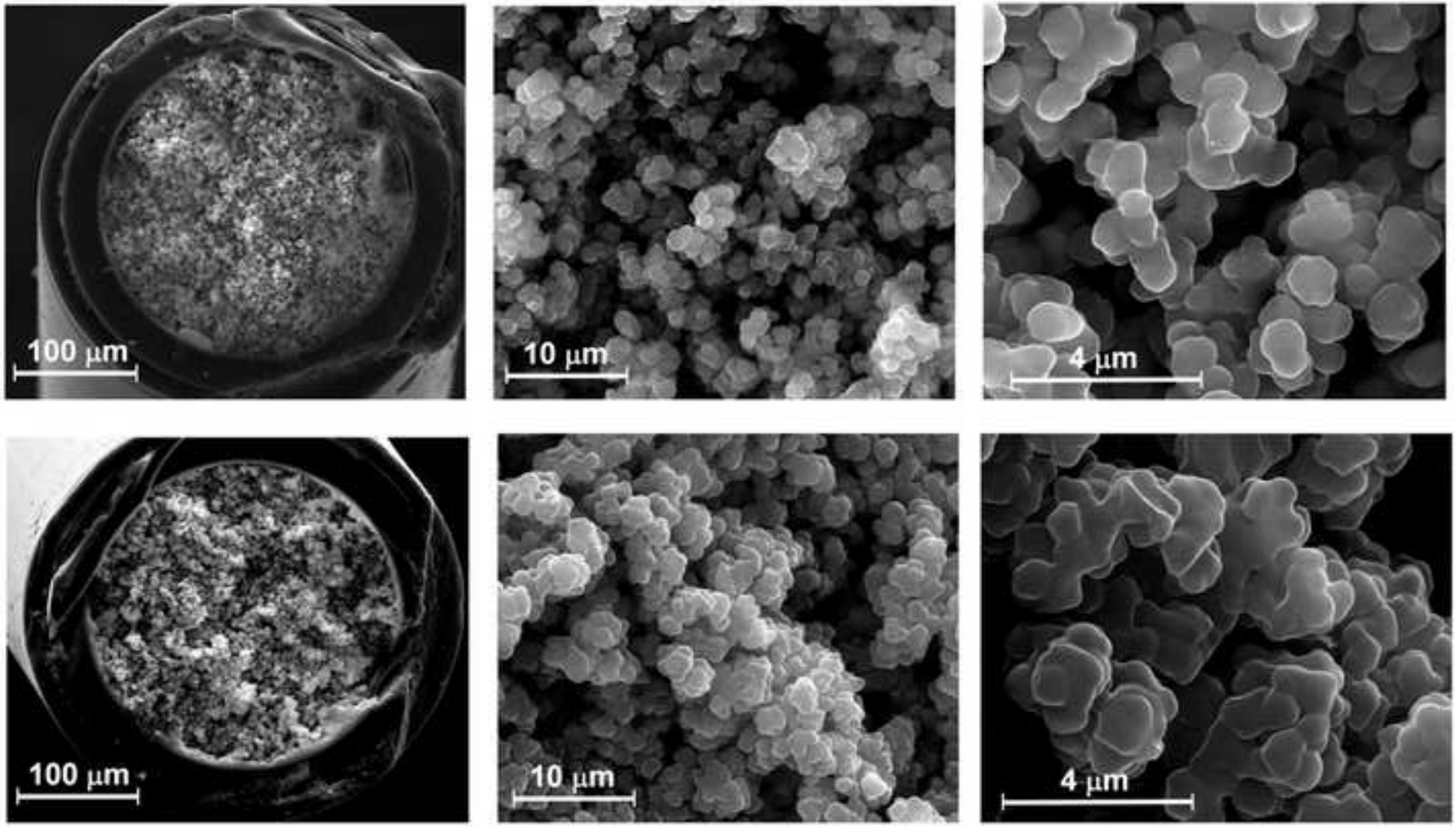

Figure

Click here to download high resolution image

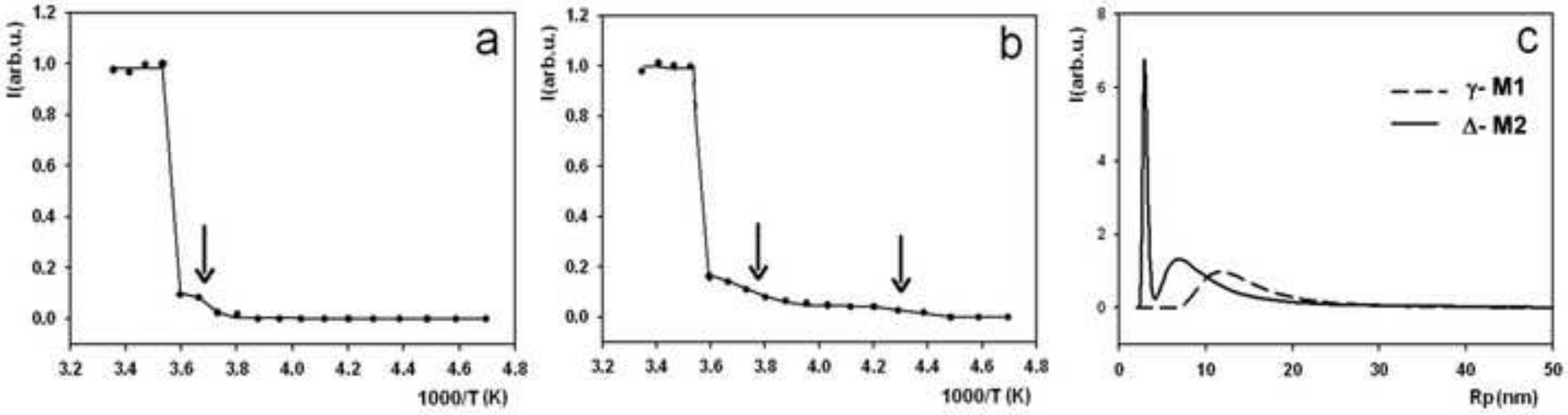

Figure

Click here to download high resolution image

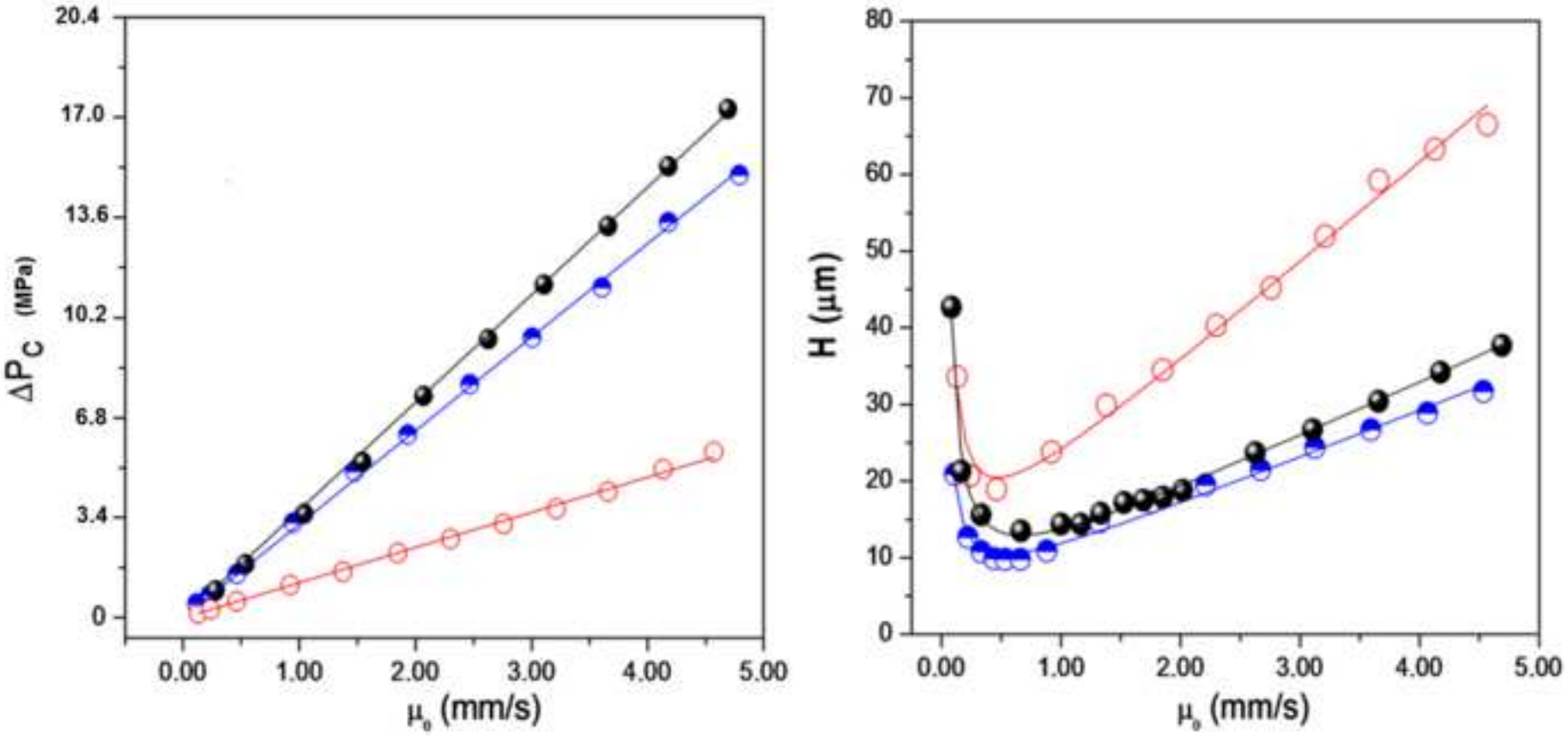

Figure
Click here to download high resolution image

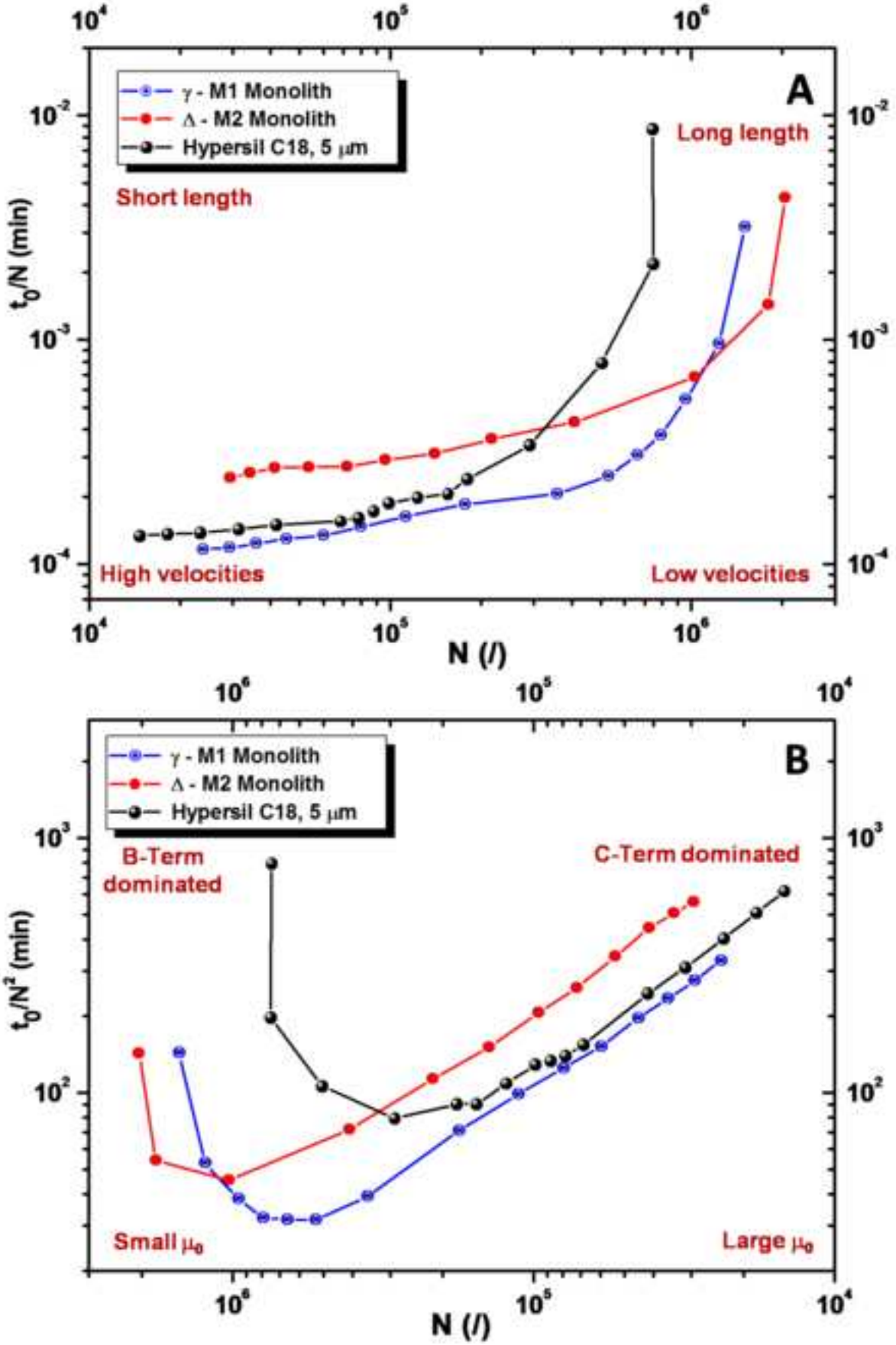

Figure

Click here to download high resolution image

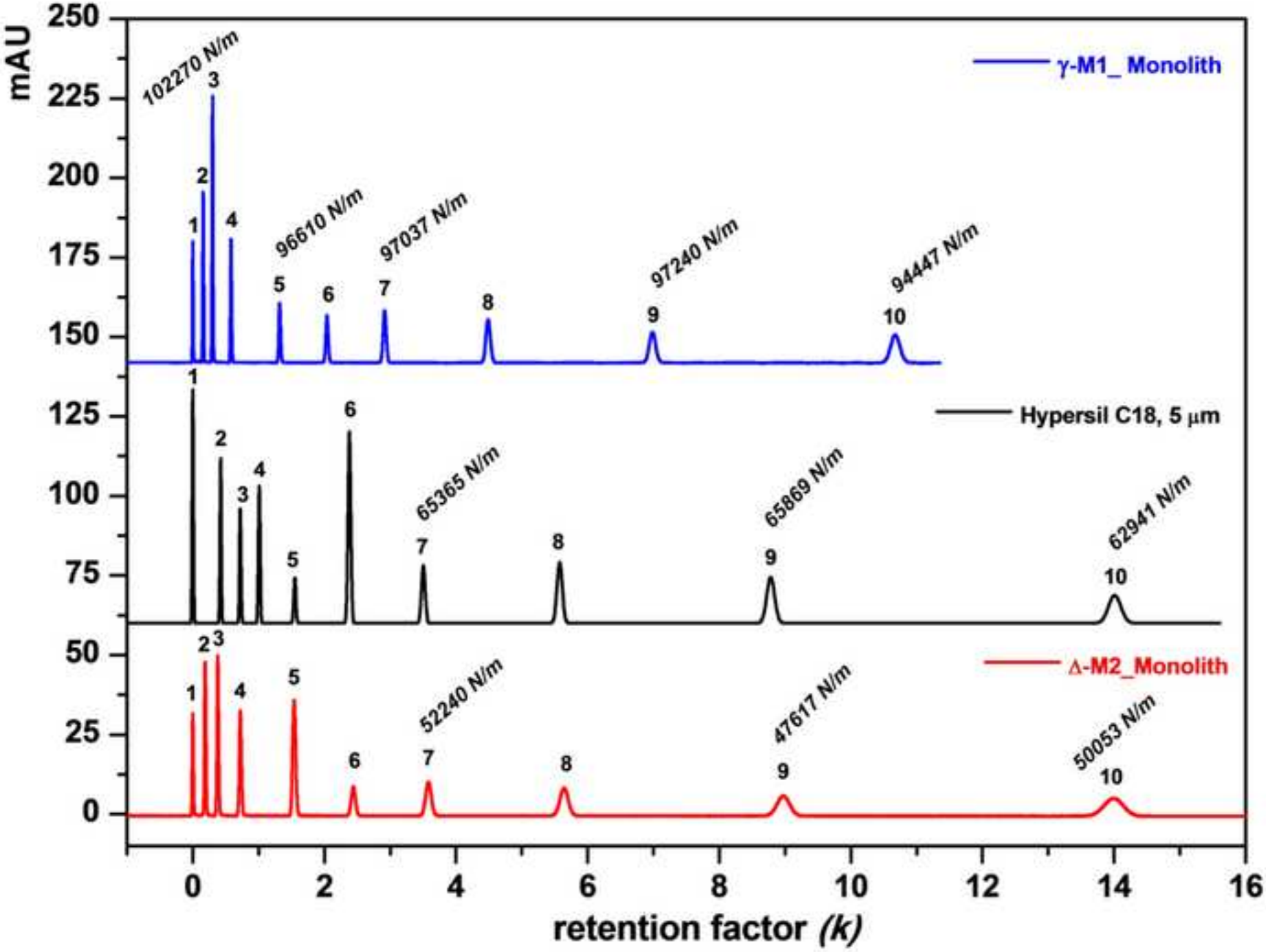

Figure

Click here to download high resolution image

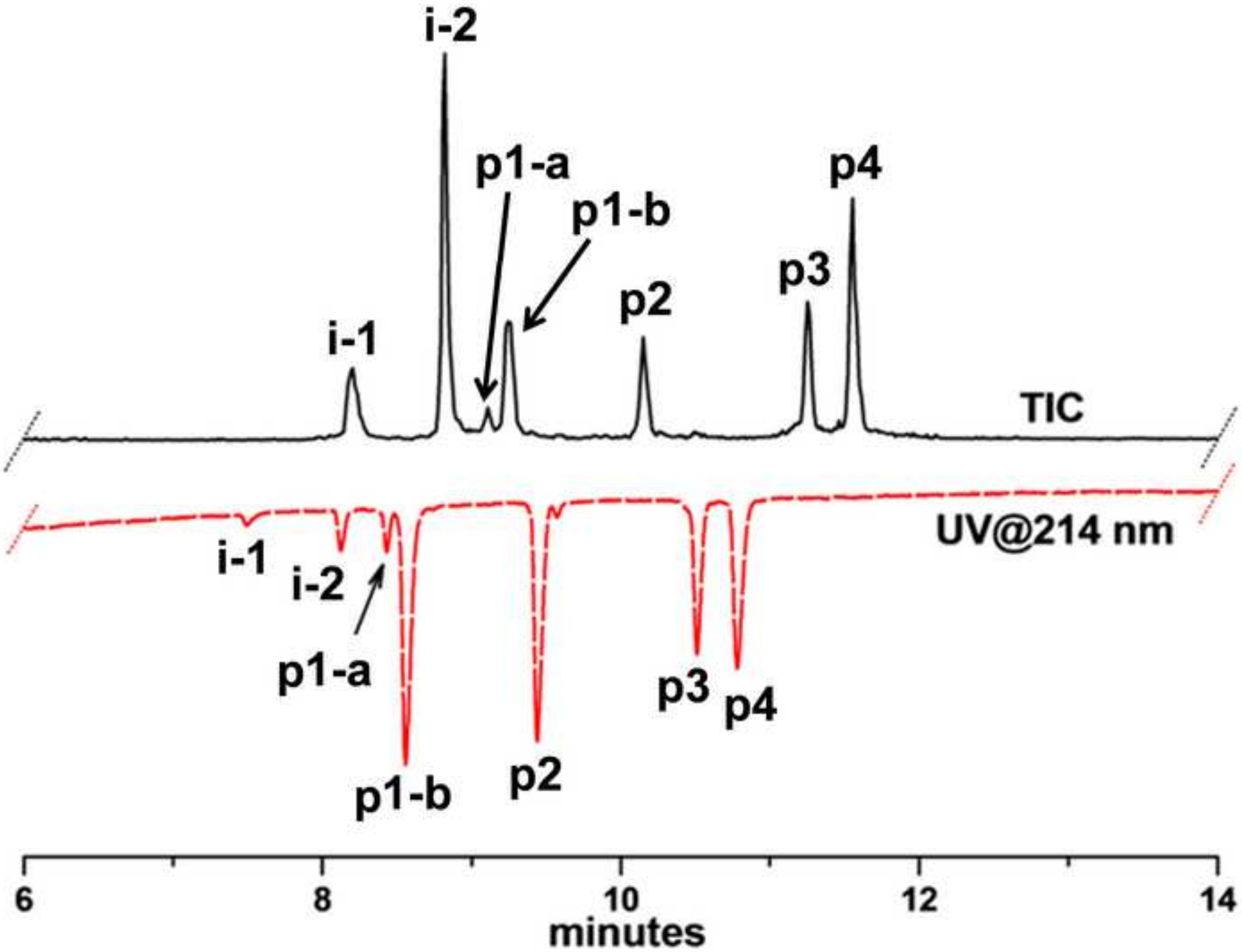

Figure

Click here to download high resolution image

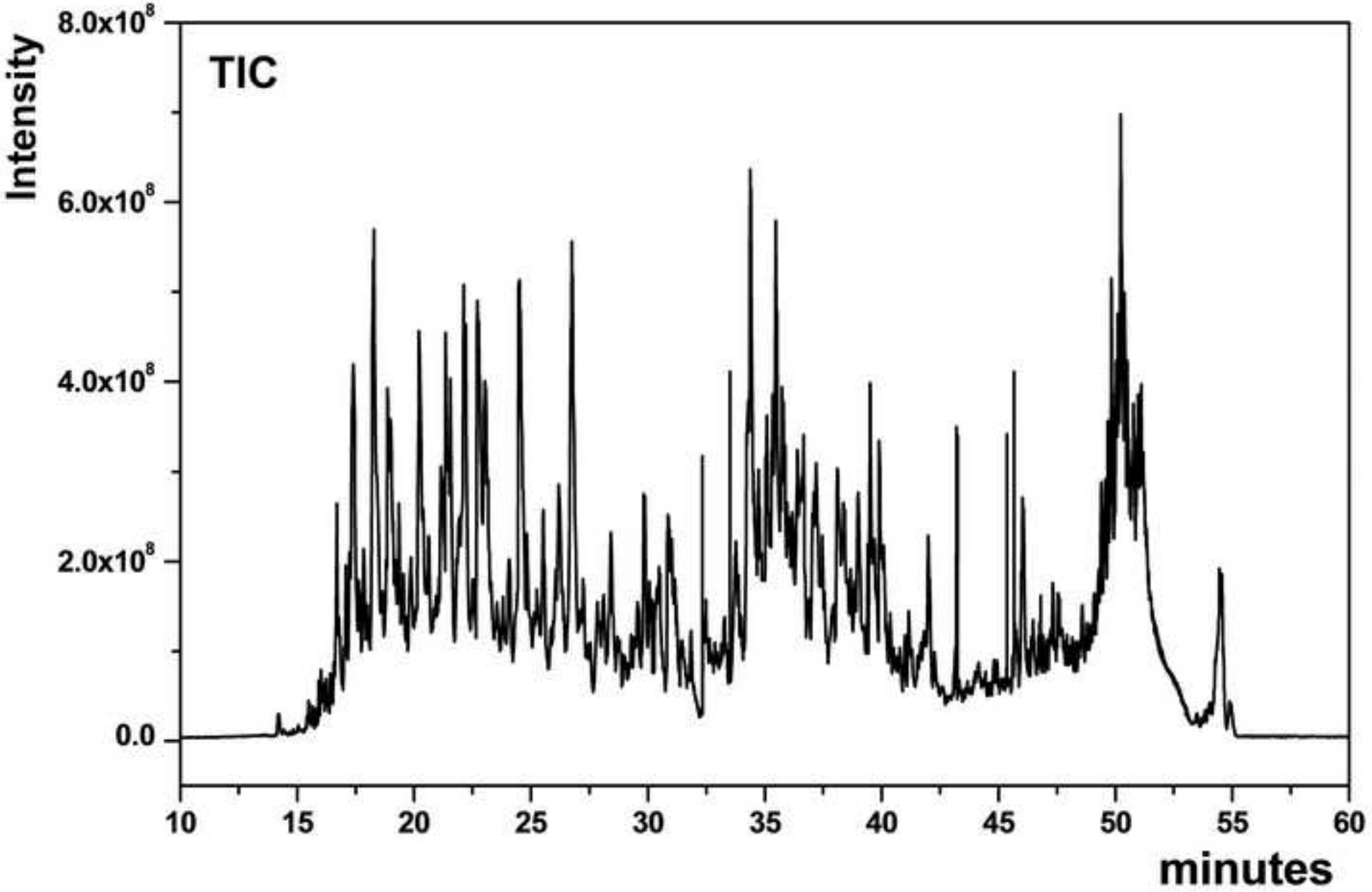

Tables

Table 1. Parameters obtained fitting IT plots of benzene-saturated networks to equation 1.

Sample	X_{ci} (K^{-1})	Δ_i (K)	I_{0i} (a.u.)
γ-M1	3.555	0.010	0.881
	3.700	0.042	0.129
Δ-M2	3.555	0.012	0.802
	3.761	0.117	0.139
	4.342	0.113	0.047

Table 2. Chromatographic parameters for columns containing monoliths γ-M1 and Δ-M2 compared to Hypersil C18, 5 µm packed column. Eluent: ACN/H_2O 60/40 (v/v), η = 0.72 cP at 25 °C; sample: benzaldehyde for kinetic inspection. K_0, K_{SF}, ε_t and d_{perm} values were obtained using uracil as unretained marker.

Capillary columns	k	Permeability ($\times 10^{-14}$ m^2)		ε_t (%)	H_{min} (µm)	N/m	μ_{opt} (mm/s)	A (µm)	B (μm^2/ms)	C (ms)	d_{perm} (µm)
		K_0	K_{SF}								
γ-M1	0.30	7.03	5.09	72.5	9.8	102270	0.525	3.97	1.71	6.21	7.12
Δ-M2	0.38	18.07	13.19	73.0	18.9	52790	0.467	8.12	2.88	13.19	11.48
Hypersil C18, 5 µm	0.72	5.90	3.55	60.1	12.9	77500	0.656	3.54	3.08	7.15	5.96

Electronic Supplementary Material (online publication only)

Click here to download Electronic Supplementary Material (online publication only): SuppInfo_JCA Monolith_R.docx